The future of global water stress: An integrated assessment*

C. Adam Schlosser, Kenneth Strzepek, Xiang Gao, Charles Fant, Élodie Blanc, Sergey Paltsev, Henry Jacoby, John Reilly and Arthur Gueneau

MIT JOINT PROGRAM ON THE SCIENCE AND POLICY of GLOBAL CHANGE

***Reprinted from**
***Earth's Future*, online first (doi: 10.1002/2014EF000238)**

Reprint 2014-16

The MIT Joint Program on the Science and Policy of Global Change combines cutting-edge scientific research with independent policy analysis to provide a solid foundation for the public and private decisions needed to mitigate and adapt to unavoidable global environmental changes. Being data-driven, the Program uses extensive Earth system and economic data and models to produce quantitative analysis and predictions of the risks of climate change and the challenges of limiting human influence on the environment—essential knowledge for the international dialogue toward a global response to climate change.

To this end, the Program brings together an interdisciplinary group from two established MIT research centers: the Center for Global Change Science (CGCS) and the Center for Energy and Environmental Policy Research (CEEPR). These two centers—along with collaborators from the Marine Biology Laboratory (MBL) at Woods Hole and short- and long-term visitors—provide the united vision needed to solve global challenges.

At the heart of much of the Program's work lies MIT's Integrated Global System Model. Through this integrated model, the Program seeks to: discover new interactions among natural and human climate system components; objectively assess uncertainty in economic and climate projections; critically and quantitatively analyze environmental management and policy proposals; understand complex connections among the many forces that will shape our future; and improve methods to model, monitor and verify greenhouse gas emissions and climatic impacts.

This reprint is one of a series intended to communicate research results and improve public understanding of global environment and energy challenges, thereby contributing to informed debate about climate change and the economic and social implications of policy alternatives.

Ronald G. Prinn and John M. Reilly,
Program Co-Directors

For more information, contact the Program office:
MIT Joint Program on the Science and Policy of Global Change

Postal Address:
Massachusetts Institute of Technology
77 Massachusetts Avenue, E19-411
Cambridge, MA 02139 (USA)

Location:
Building E19, Room 411
400 Main Street, Cambridge

Access:
Tel: (617) 253-7492
Fax: (617) 253-9845
Email: ***globalchange@mit.edu***
Website: ***http://globalchange.mit.edu/***

AGU PUBLICATIONS

Earth's Future

RESEARCH ARTICLE

10.1002/2014EF000238

Key Points:
- Integrated global water-resource projections resulting from global change
- Additional 1 billion people may live within high stress stress regions by 2050
- Developing nations affected strongly by socio economic growth

Corresponding author:
C. A. Schlosser, casch@mit.edu

Citation:
Schlosser, C. A., K. Strzepek, X. Gao, C. Fant, É. Blanc, S. Paltsev, H. Jacoby, J. Reilly, and A. Gueneau (2014), The future of global water stress: An integrated assessment, *Earth's Future, 2*, doi:10.1002/2014EF000238.

Received 4 FEB 2014
Accepted 23 MAY 2014
Accepted article online 28 MAY 2014

The future of global water stress: An integrated assessment

C. Adam Schlosser[1], Kenneth Strzepek[1], Xiang Gao[1], Charles Fant[1], Élodie Blanc[1], Sergey Paltsev[1], Henry Jacoby[1], John Reilly[1], and Arthur Gueneau[2]

[1]Joint Program on the Science and Policy of Global Change, Massachusetts Institute of Technology, Cambridge, Massachusetts, USA, [2]International Food Policy Research Institute (IFPRI), Washington, District of Columbia, USA

Abstract We assess the ability of global water systems, resolved at 282 assessment subregions (ASRs), to the meet water requirements under integrated projections of socioeconomic growth and climate change. We employ a water resource system (WRS) component embedded within the Massachusetts Institute of Technology Integrated Global System Model (IGSM) framework in a suite of simulations that consider a range of climate policies and regional hydroclimate changes out to 2050. For many developing nations, water demand increases due to population growth and economic activity have a much stronger effect on water stress than climate change. By 2050, economic growth and population change alone can lead to an additional 1.8 billion people living under at least moderate water stress, with 80% of these located in developing countries. Uncertain regional climate change can play a secondary role to either exacerbate or dampen the increase in water stress. The strongest climate impacts on water stress are observed in Africa, but strong impacts also occur over Europe, Southeast Asia, and North America. The combined effects of socioeconomic growth and uncertain climate change lead to a 1.0–1.3 billion increase of the world's 2050 projected population living with overly exploited water conditions—where total potential water requirements will consistently exceed surface water supply. This would imply that adaptive measures would be taken to meet these surface water shortfalls and include: water-use efficiency, reduced and/or redirected consumption, recurrent periods of water emergencies or curtailments, groundwater depletion, additional interbasin transfers, and overdraw from flow intended to maintain environmental requirements.

1. Introduction

Concern about projected global climate change and other pressures on the natural, managed, and built environments have focused particular attention on the availability and reliability of water supplies in the coming decades. As a result, there is a growing need for modeling and analysis tools that can provide quantitative insights into these issues while representing the full integration of the climate system with its socioeconomic drivers, hydrology and water supplies, water-use sectors, and management strategies. In response to the inadequate understanding of critical interactions between natural processes and human activities over a wide range of spatial and temporal scales, a subgroup of the International Group of Funding Agencies for Environmental Change Research includes as a key element of its "Belmont Challenge" [(*IGFAGCR*), 2011] the need, "to deliver knowledge needed for action to avoid and adapt to detrimental environmental change." Additionally, they selected freshwater security as one of five priority foci, and the need for integrated research. This need is influenced by natural hydrometeorological processes as well as socioeconomic interdependencies, such as land use or water extraction (for agriculture, energy, and industry), which in turn are governed by patterns of consumption, production, and/or population change. While global water modeling tools have been developed [e.g., *Hirabayashi et al*., 2008; *Döll and Zhang*, 2010; *Gosling et al*., 2010; *Fung et al*., 2011; *Okazaki et al*., 2012; *Tang and Lettenmaier*, 2012; *Arnell and Gosling*, 2013] most of the experimentation studies conducted with these models have been driven by exogenous climate forcing that is disconnected from consistent socioeconomic pathways. Therefore, they fall short of the Belmont Challenge call for understanding "critical interactions between natural processes and human activities."

In response to this challenge, we have expanded the Massachusetts Institute of Technology (MIT) Integrated Global System Model (IGSM) framework to include a water resource system (WRS) component [*Strzepek et al*., 2013]. Here, the IGSM-WRS is applied at global scale to assess future water stress, resolved

for 282 interlinked basins or Assessment Subregions (ASRs). Water resources and the ability to manage them effectively will be shaped by both human requirements for withdrawal from natural sources and changes in regional climate. This analysis is designed to isolate these two influences in simulations to 2050. To quantify the influence of economic growth alone, simulations compare water stress under economic growth with a no-growth scenario, holding climate at its historical condition. To understand the role of climate, a no-growth economy is assumed and water stress is assessed under different scenarios of climate change reflecting both regional uncertainty and climate policy. Two policy cases are used: one with unconstrained emissions and the other imposing a 560 ppm CO_2-equivalent stabilization target. The IGSM framework allows for a pattern-scaling approach [*Schlosser et al*., 2012] that can explore the impact of uncertain regional climate change. Therefore, we consider two patterns of climate change, obtained from the pool of climate models in the coupled model intercomparison project phase 3 [CMIP3, *Meehl et al*., 2007]. We denote the first pattern as relatively "wet" and the other as relatively "dry" based on a global land-only analysis of climate moisture index [CMI, *Willmott and Feddema*, 1992] trends in response to increased greenhouse gases [*Strzepek and Schlosser*, 2010]. The CMI illustrates the relationship between potential plant water demand and available precipitation and ranges from −1 to +1, with wet climates showing positive CMI, and dry climates negative CMI. The land-only focus in the assessment of CMI trends was performed to emphasize the range of precipitation and evapotranspiration outcomes that affect the water balance of river basins. Finally, the total effect of these influences is evaluated in simulations imposing both economic growth and climate change.

In Section 2 we summarize the model applied in the analysis and the experiments used to separate out the various contributors to increasing stress on water systems. Section 3 presents the key results. In Section 3.1, we establish a baseline for comparison of the various influences and present results for runoff and water stress by ASR for a recent period. Section 3.2 presents results of the separate effects of economic growth and climate change on water stress. Finally, in Section 3.3 we show the results for their combined effects, via two concepts of water stress. Section 4 concludes with a discussion of applications and then steps in this research and assessment activity.

2. Models and Methods

2.1. The IGSM-WRS Model

The focus of this numerical experimentation and analysis is to evaluate the effect of socioeconomic growth and climate changes on the future availability of water for management purposes at large watersheds, or ASRs, across the globe. *Strzepek et al*. [2013] provides a complete description of the natural and managed components of the IGSM-WRS (Figure 1), whereas the current study briefly describes the key elements. The Emissions Prediction and Policy Analysis (EPPA) component of the IGSM provides the WRS with economic drivers (population, GDP) for the estimation of municipal and industrial water demand. As described in the study by *Strzepek et al*. [2013], these algorithms that use GDP and population to estimate water demand are strongly nonlinear in order to depict rapid growth in demand for developing economies as well as increases in water-use efficiency as nations become more developed. The EPPA also provides greenhouse gas, aerosol, as well as other pollutant emissions to the MIT Earth System Model (MESM). From the MESM, runoff is determined from the Community Land Model Version 3.5 [*Oleson et al*., 2004] employed within the IGSM's Global Land System [*Schlosser et al*., 2007]. The simulated runoff from CLM is then calibrated [as shown by *Strzepek et al*., 2013] such that each ASR contains as realistic natural flow conditions as possible. The CliCrop Model [*Fant et al*., 2012] calculates irrigation demands explicitly for a variety of crops. All of these demands and surface water supply are fed into the water system management (WSM) in order to optimize the routing of water supply across all of the ASRs. The resultant routing is then analyzed via a water stress indicator (described in Section 2.3).

The impact of the plausible range in regional climate change resulting from each of these emission scenarios is considered using the IGSM outputs and a method [*Schlosser et al*., 2012] that uses observationally based downscaling patterns (to represent the current climate) combined with scaled patterns of human-forced climate change derived from the CMIP [*Meehl et al*., 2007]. For the simulations described below, the IGSM is employed using its median values of both climate parameters

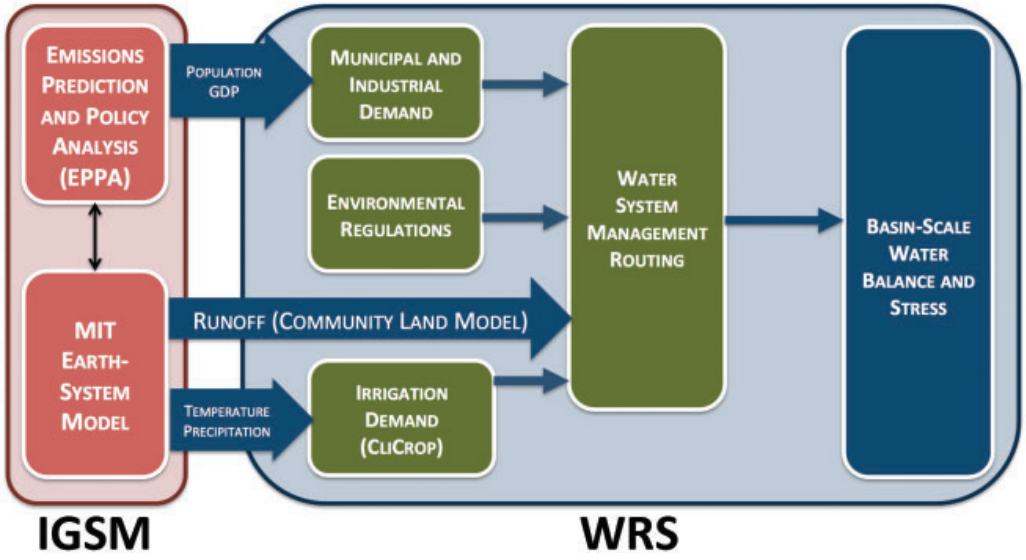

Figure 1. Schematic of IGSM-WRS. Shown are the connections between the socioeconomic and earth system model components of the Integrated Global System Model (IGSM) framework and the water resource system (WRS) component. The water system management module optimizes the ability of routed water supply (i.e., runoff and inflow) to meet the demands across all ASRs. See text for further details.

(climate sensitivity, ocean uptake, and aerosol effects) and economic parameters [*Webster et al*., 2012].

For this study, the WRS is configured to represent 282 ASRs over the globe (Figure 2). The ASRs are defined by major river basins or parts of river basins contained within a country. For example, the Nile river basin is divided into six ASRs as the Blue Nile begins in Ethiopia (at Lake Tana), the White Nile starts in Uganda (at Lake Victoria), and they converge in Sudan to form the Nile River, which then discharges into the Mediterranean Sea while crossing Egypt. A comprehensive ASR listing is provided in *Strzepek et al*. [2013] as well as the basin-level processes of the natural and managed water system that are represented by the model. Briefly, for each ASR, available reservoirs are aggregated into a single storage unit that is fed by runoff and input from upstream ASRs and that serves human water sector requirements and a required environmental flow. Nonirrigation requirements—for municipal, industrial, and livestock uses—are driven by socioeconomic factors on the assumption that they are not significantly influenced by climate. In addition, irrigated lands do not feedback to the atmosphere, but we note that the total surface area of irrigated land represents a small fraction (less than 2%) of the globe [e.g., *United Nations World Water Assessment Programme* (*WWAP*), 2014]. Furthermore, based on recent evidence over the past decade, growth in global irrigated land area has slowed considerably [e.g., *Siebert et al*., 2005, 2013; *Thenkabail et al*., 2008] even though global food production has steadily increased [e.g., *FAO*, 2013]. This indicates that rising global food demand is being met by increased rainfed agriculture and intensification of existing irrigated land. Furthermore, given the complexity of interactive socioeconomic drivers, environmental pressures, as well as global and national governance that will affect future decisions regarding irrigation expansion [i.e., new dams and reservoirs, e.g., *World Commission on Dams* (*WCOD*), 2000] the irrigated area is held constant in these experimental simulations (equal to current estimates from FAO and IFPRI—see *Rosegrant et al*., 2008], and we focus on whether there is adequate water to meet changing needs under changes in ASR scale socioeconomic activity and climate.

2.2. Model Experiments

A suite of simulations is used to explore the key drivers of water stress within each of the 282 basins of the global WRS configuration used herein. Table 1 provides a summary of cases that spans both growth assumptions (no-growth and two future growth scenarios) and different scenarios of the influence of climate (alternative greenhouse gas control policies as well as a range of climate change patterns as

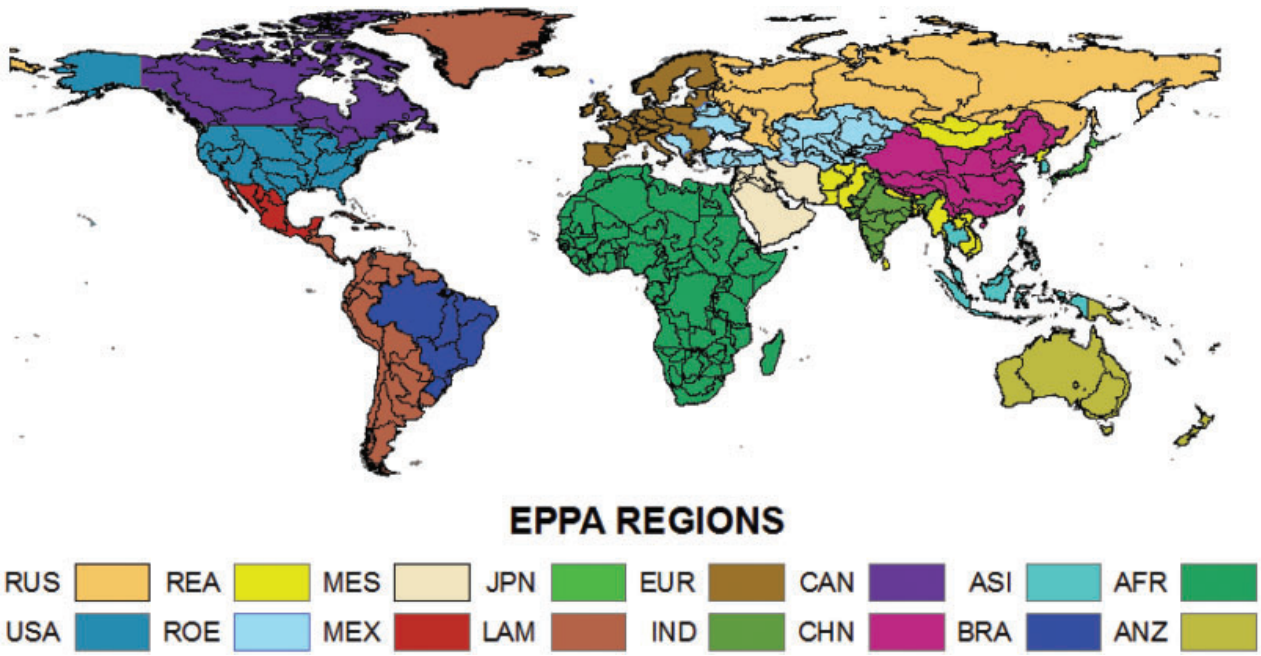

Figure 2. Schematic of IGSM-WRS. Black contours delineate the assessment subregions (ASRs) defined for the water resource system (WRS) within the IGSM-WRS framework. The color shading indicates the economic regions that are resolved from the Emissions Prediction and Policy Analysis (EPPA) model.

Table 1. Climate Change Pattern and Socioeconomic Scenarios[a]

	No-Growth (NG)	Unconstrained Emissions Growth (UCE)	Level 1 Stabilization Growth (L1S)
Historic climate (HC)	Baseline	UCE-HC	L1S-HC
UCE with DRY pattern	NG-UCE-DRY	UCE-DRY	
UCE with WET pattern	NG-UCE-WET	UCE-WET	
L1S with DRY pattern	NG-L1S-DRY		L1S-DRY
L1S with WET pattern	NG-L1S-WET		L1S-WET

[a]The table provides a guide to the cases used in the analysis. The columns depict the branches of simulations performed to assess the impact of three economic pathways: no-growth (NG), unconstrained emissions (UCE), and a Level 1 stabilization (L1S) scenario that stabilizes CO_2-equivalent concentrations at 560 ppm by 2100. Two climate model patterns are used from the IPCC CMIP3 archive in the pattern scaling of IGSM projections, and were selected according to their relatively wet (WET) and dry (DRY) trending climate moisture indices averaged globally over land only.

determined by CMIP3 climate models. They thus form four groups, which guide the layout of results in the discussion below.

1. *Baseline*. To provide a basis for comparing the effects of socio-economic growth and climate change over time, a baseline scenario involves historic climate (HC), which is based on the simulated twentieth century climate from the IGSM [e.g., *Sokolov et al*., 2005] downscaled to a 2° × 2° gridded resolution using observations [*Schlosser et al*., 2012], but with no growth (NG). This condition is explored in Section 3.1.
2. *Socio-economic growth effects*. To isolate the effect of socio-economic growth (hereafter, referred to as "growth" for brevity) on water conditions, a set of scenarios (top line in Table 1) impose HC and explore the change with different growth conditions. They include no-growth (Baseline) and growth with unconstrained emissions (UCE) analyzed by *Sokolov et al*. [2005]. The growth rates, by EPPA region, assumed in this case are provided in Table 2, and these rates are assumed to hold for the ASRs within

Table 2. Economic Growth Assumptions[a]

Major Regions	Region	GDP (trillions US$) 2000	GDP (trillions US$) L1S 2050	GDP (trillions US$) UCE 2050	Average Annual GDP Growth Rate (%) L1S	Average Annual GDP Growth Rate (%) UCE
Developed	ANZ	0.57	2.51	2.58	3.0	3.1
	CAN	0.71	2.81	2.95	2.8	2.9
	ROE	0.34	1.49	1.48	3.0	3.0
	EUR	10.26	37.57	37.96	2.6	2.7
	JPN	6.07	23.77	24.06	2.8	2.8
	USA	9.52	38.54	38.38	2.8	2.8
Other G20	CHN	1.05	8.04	7.61	4.2	4.0
	RUS	0.51	2.72	2.97	3.4	3.6
	BRA	1.08	5.13	5.09	3.2	3.1
	IND	0.49	2.06	2.02	2.9	2.8
	MEX	0.40	1.32	1.44	2.5	2.6
Developing	AFR	1.01	3.15	4.42	2.3	3.0
	ASI	0.23	1.12	1.11	3.2	3.2
	LAM	1.75	7.89	9.19	3.0	3.4
	MES	0.61	1.86	2.52	2.2	2.9
	REA	1.20	4.32	4.62	2.6	2.7

[a]Gross domestic product (GDP) in 2050 for the geographical regions resolved by the Emissions Prediction and Policy Analysis (EPPA) model (see Figure 1). Absolute values of GDP (in constant 2000 US$) are shown for 2000 as well as the values attained for the two socioeconomic scenarios considered (unconstrained emissions, UCE, and Level 1 Stabilization, L1S, see Table 1 and text for details). These changes are calculated and shown as average annual growth rates, accordingly.

the region. This case is designated UCE-HC. An additional case, designated L1S-HC, is formulated applying the growth that is projected under a global policy to restrain global emissions to the Level 1 scenario (L1S) developed for the U.S. Climate Change Science Program [*Clarke et al*., 2007]. The L1S scenario imposes a target of 560 ppm CO_2-equivalent concentrations by 2100. Meeting these targets lowers economic growth, especially in some parts of the developing world: primarily in Africa, the Middle East, and Central and South America, also shown in Table 2 [*Webster et al*., 2012]. The effects on water requirements of these different growth assumptions are discussed in Section 3.2.1. The UCE and L1S scenarios use the same global population projection, the United Nations' medium-variant projection, [*United Nations*, 2013]. To be consistent with the IGSM uncertainty formulation, socioeconomic projections are provided by EPPA regions (Figure 2). To provide these population projections at the ASR scale, the EPPA regions' rate of population changes are mapped to the ASR regions that fall within each EPPA region. The ASR-based population projections use the growth rates from EPPA with the current populations provided at the ASR-level developed by IPFRI [*Rosegrant et al*., 2008] (Figure 3).

3. *Climate change effects*. The left column of the table shows cases designed to address the effect of uncertainty in regional climate change. All are studied on the assumption of NG effects on water demands (the emission scenarios driving these climate effects reflect economic growth). Through a pattern-scaling method developed by *Schlosser et al*. [2012] and employed in other studies within the IGSM framework [e.g., *Gao et al*., 2013; *Strzepek et al*., 2013], the IGSM-WRS was configured with two pattern-scaling kernels of regional climate outcomes under each of the socioeconomic/emission scenarios (UCE and L1S). These pattern change kernels were derived from the CMIP3 climate models. As previously mentioned, two patterns were chosen to reflect the "driest" (DRY) and the "wettest" (WET) changes over land as determined by their CMI trends through the 21st century [*Strzepek and Schlosser*, 2010]. It is worthwhile to note that this selection is based on the moisture index over all land, and thus these are not necessarily the wettest or driest pattern for every ASR. The resulting $2^\circ \times 2^\circ$ set of cases, all

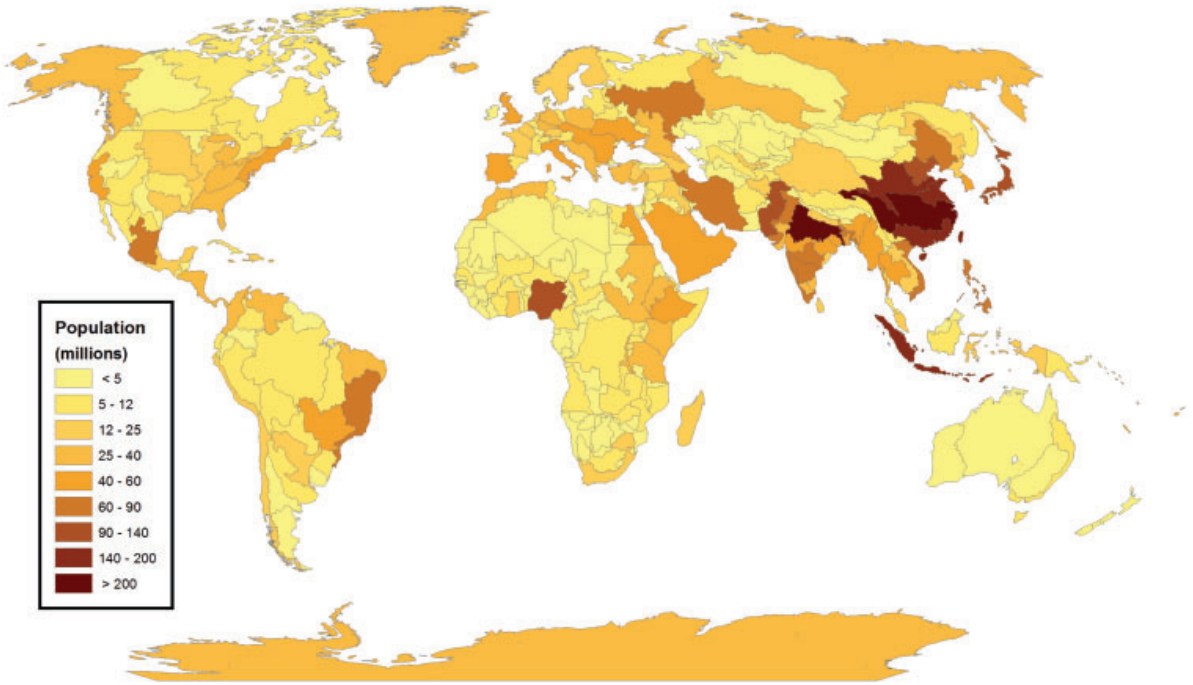

Figure 3. Global population in 2010. Global distribution of population (in millions) projected onto the assessment subRegions (ASRs) of the WRS water management network of river basins. As described in the text, the global population projections for the IGSM UCE and L1S scenarios (to 2050) are supplied at the EPPA region, and are then downscaled proportionally to the ASRs according to the 2010 population distribution shown here.

with no-growth (NG-UCE-WET, NG-UCE-DRY, NG-L1S-WET, and NG-L1S-DRY) are discussed in Section 3.2.2.

4. *Combined growth and climate change effects*. The combined effect of growth and climate is explored using the four cases in the lower-right quadrant of the table. The behaviors of the two climate change patterns (WET and DRY) are formulated under both unconstrained growth (UCE-WET and UCE-DRY) as well as for the Level 1 climate policy growth (L1S-WET and L1S-DRY). The results for these combined effects are presented in Section 3.3

The IGSM-WRS is integrated to 2050 for all cases. The analyses presented below will focus on the ability of the ASRs to meet the water demands [*Strzepek et al*., 2013] and the relative stress that these demands place on renewable surface water as well as water that is available within the managed system.

2.3. Measure of Water Stress

Many indices have been developed to quantify water "stress" over a region or basin of interest [e.g., *Brown and Matlock*, 2011], and for this study we have chosen a metric that requires variables that can be directly extracted from the WRS, and the metric has also been evaluated and employed in previous studies with the IGSM-WRS [*Blanc et al*., 2013; *Strzepek et al*., 2013]. We define a water stress index (WSI) similar to that developed by *Smakhtin et al*. [2005]. It is based on the input water flows, from surface runoff and upstream ASRs, and desired withdrawals and thus is a measure of the pressure that human water uses exert on renewable surface fresh water. It is calculated, for every ASR, as the ratio of its mean annual total water requirements (TWR) to the mean annual runoff (RUN) generated within the ASR plus inflow (INF) from any upstream ASR that flows directly into it,

$$\mathrm{WSI} = \frac{\mathrm{TWR}}{\mathrm{RUN} + \mathrm{INF}} \tag{1}$$

as described by *Strzepek et al*. [2013], for all water sectors except irrigation (i.e., municipal and industrial), water requirements included in TWR are represented by consumptive use. On the basis of the assumption that any return flow (withdrawal in excess of consumption) is likely returned to the ASR storage within the month. This assumption is not appropriate for irrigation because return flow, which may be substantial,

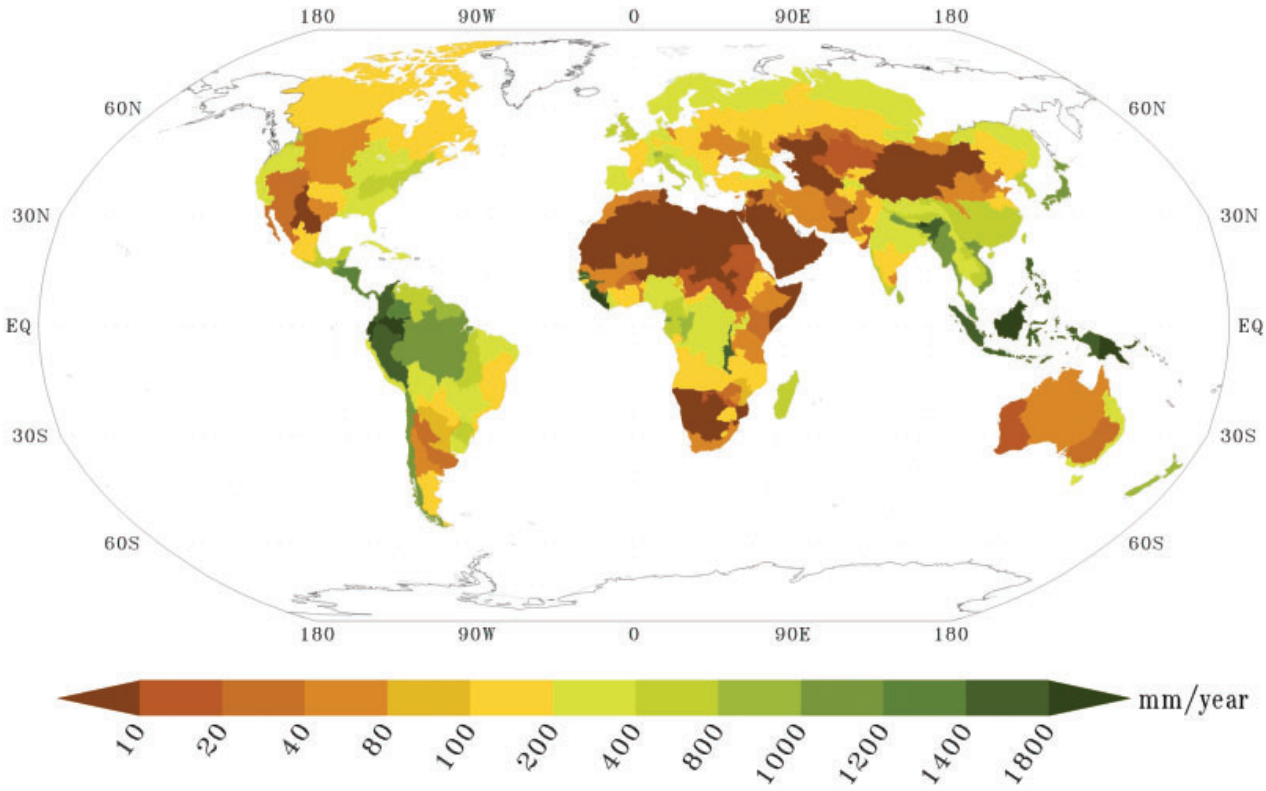

Figure 4. Annual runoff. Global distribution of annual runoff (mm/year) as simulated by CLM from a historical climate run of the IGSM and projected onto the assessment subregions (ASRs) of the WRS water management network of river basins. The simulated ASR values are an average for the years 1981–2000.

may not be returned to the ASR storage immediately. The inflow into any given ASR is a consequence of flow regulated from upstream ASRs, and therefore WSI is an evaluation metric of the managed water system as simulated by WRS. Irrigation receives its total withdrawal, with its return flow that may be substantial, credited to the downstream ASR [see *Strzepek et al*., 2013 for details]. We also characterize the severity of water stress according to *Smakhtin et al*. [2005], which classifies an ASR's water use as slightly exploited when WSI < 0.3; moderately exploited when $0.3 \leq$ WSI ≤ 0.6; heavily exploited when $0.6 \leq$ WSI ≤ 1; overly exploited when $1 \leq$ WSI < 2; and extremely exploited when WSI ≥ 2. Similar WSIs are computed in other studies and generally consider a threshold of 0.4 to indicate severe water limitation [e.g., *Vörösmarty et al*., 2000; *Wada et al*., 2011].

3. Results

3.1. Baseline Scenario

The baseline is simulated with twentieth century climate and current (i.e., recent year) economic conditions. Figure 4 maps the WRS annual runoff estimate within each ASR, averaged over the period 1980–2000. The Amazon Basin, Southeast Asia, and parts of Equatorial Africa and Indonesia stand out as showing the highest annual rates of runoff. In addition, the stark east–west contrast of runoff over the United States can be observed. Among the lowest rates of runoff are those over most of Northern Africa, the Middle East, central Australia, and Mongolia.

WSI for the same historical period is shown in Figure 5. Areas of highest water stress are aligned across many of the regions of low runoff and arid conditions. Additionally, substantial stress can be observed in the southwestern portions of the United States, southeastern Australia (the Murray–Darling Basin), and interior portions of South Africa and Namibia. By this measure, most of the ASRs across the globe fall within the slightly stressed characterization. However, of particular concern are the regions shaded within the heavily to extremely stressed conditions. Many of these ASRs correspond to regions of very

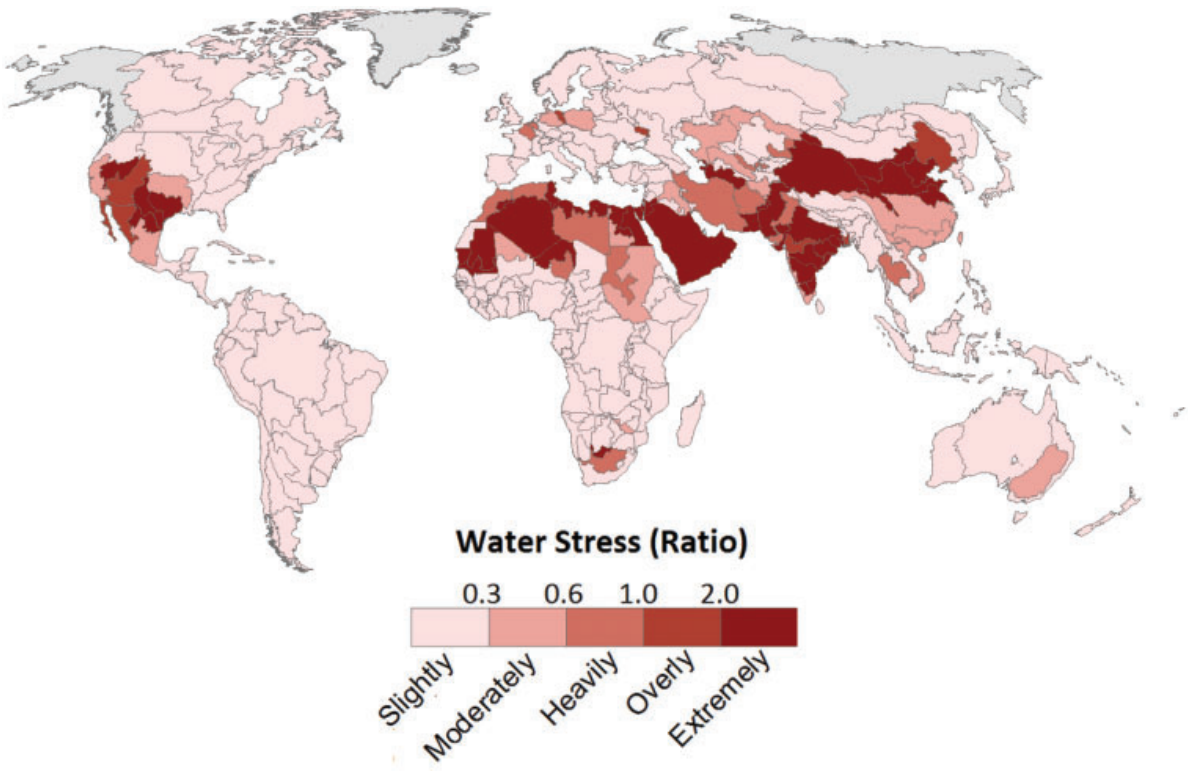

Figure 5. Water stress. Shown is the global distribution of water stress index (WSI) by assessment subregions (ASRs) as simulated by WRS from a historical climate run of the IGSM-WRS (i.e., the baseline in Table 1). The simulated values are an average for the years 1981–2000 of the historical baseline simulation (see Table 1 and corresponding text). The shading levels also denote the Smakhtin et al. (2005) stress categories: WSI < 0.3 is slightly exploited, 0.3 ≤ WSI < 0.6 is moderately exploited, 0.6 ≤ WSI < 1 is heavily exploited, 1 ≤ WSI < 2 is overly exploited, and WSI ≥ 2 is extremely exploited.

low runoff (Figure 4). Exceptions to this characterization are observed for ASRs located in India, showing significant runoff but extreme overexploitation of water resources. This is a result of the combined effects of India's large population and developing economy—which both contribute toward high water demand. This high value of WSI is also a consistent reflection of India's extensive groundwater extraction. A similar global baseline WSI result for the IGSM-WRS was previously evaluated in the study by *Strzepek et al*. [2013, Figures 8 and 9] against the FAO AQUASTAT WSI result and found to have a regression of slope 1.09 and R^2 of 0.96. Conducting the same regression evaluation with the baseline result shown in Figure 5, we obtain a slope of 1.16 and R^2 of 0.82.

3.2. Autonomous Effects of Economic Growth and Climate Change

3.2.1. Economic Growth

One set of simulations supports an assessment of the effect of economic growth from an unconstrained emission pathway (UCE) in contrast to a Level 1 climate policy (L1S) if the historical climate (HC) conditions are assumed to remain steady to 2050. A comparison of the UCE-HC case is presented with the baseline in Figures 6a and 6b. Figure 6a shows the level of water stress under the baseline scenario, aggregated to the global level. In this global aggregation, the ASRs are weighted by total water requirement. The effects of climate variability are observed in both cases and typically result in global WSI swings of ±1%. However, the effect of unconstrained socioeconomic growth is salient (Figure 6b) with respect to associated climate variation and implies that an increase in global WSI of 6% can result from economic growth alone.

Figure 7 shows, for the UCE-HC case, the change in nonagricultural water consumption by ASR over the period 2001–2010 to 2041–2050. These changes in demand contribute to the global WSI increase observed in Figure 6b. The largest, widespread relative changes occur over much of Africa and highlight the effects of extensive growth anticipated for these developing nations. Furthermore, the Middle East and many ASRs over Asia show increases in water requirements that exceed 100%. In contrast, benign

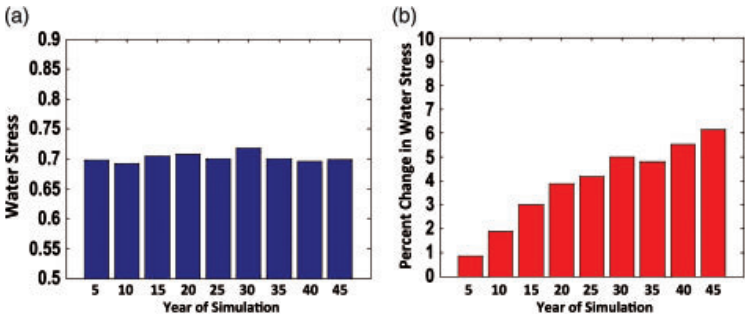

Figure 6. Global water stress. Shown are time series of globally averaged water stress index, WSI (unitless), simulated by the IGSM-WRS framework. Global values are obtained by weighting each ASR according to its total annual withdrawal. The plot shows successive 5 year averages. In panel a), the bars represent simulated water stress as a result of the historical climate conditions (Baseline case in Table 1) simulated by the IGSM. Panel b) presents the relative change in water stress, given as a percentage from the corresponding baseline value, that results from a sensitivity run where the trends in global, human water demands are based on the UCE IGSM scenario (first 50 years of the 21st century) are added onto the historical time series WRS inputs (case UCE-HC in Table 1). In both simulation results shown, the (historical) climate forcing is identical, and thus the difference plot (right panel) represents the impact of additional, unconstrained human water demand on water stress over the 50 year simulation.

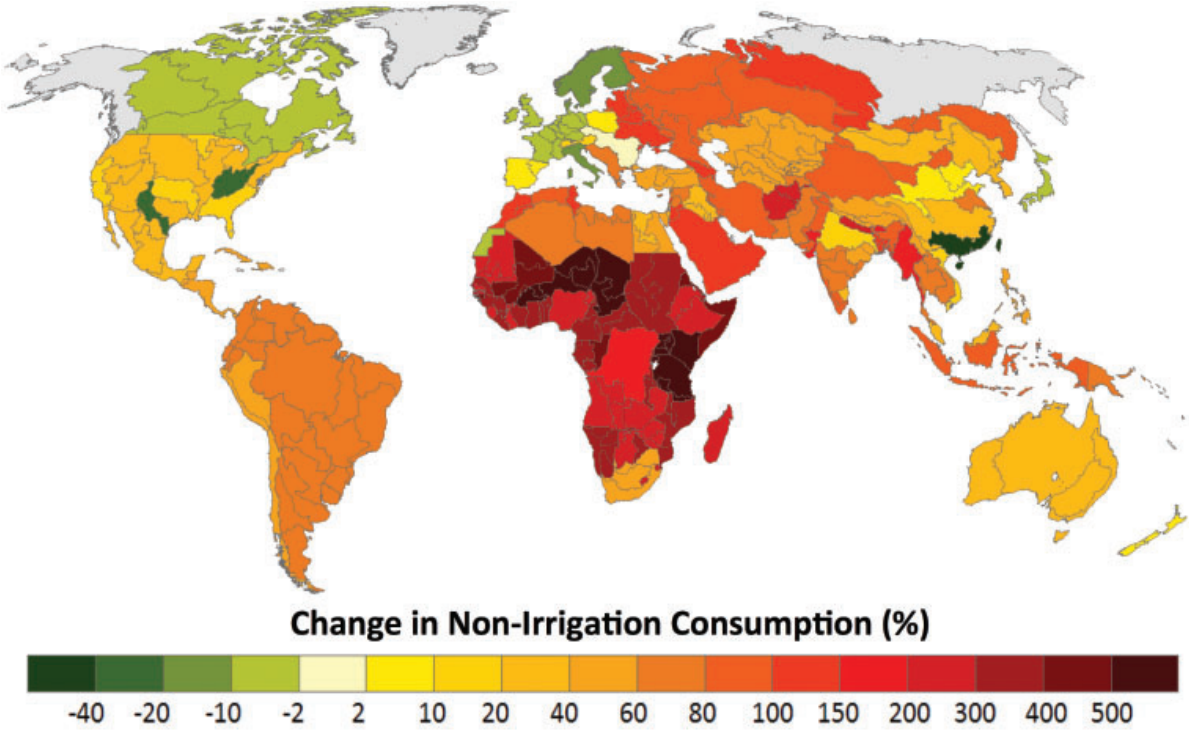

Figure 7. Change in nonirrigation water consumption by ASR. Percentage change in ASR nonirrigation water demand from 2001–2010 to 2041–2050, between the baseline and UCE-HC scenarios shown at the ASR levels. The UCE-HC scenario only considers changes in water demand as a result of economic growth factors—and climate conditions are held fixed to the historic conditions. Positive values indicate that the UCE-HC conditions are increasing nonirrigation water requirements.

changes or even reductions in nonirrigation consumption occur over much of Europe, North America, and Australia.

This difference in consumption changes between more and less developed regions is also evident when results are aggregated to the developed G20 countries and the remaining developing nations (Figure 8a). Water requirements of the developed world are relatively insensitive to socioeconomic growth in either the UCE or the L1S scenarios. Among these nations, the United States shows the largest change in water demand with an increase of approximately 17% for either the UCE or L1S scenario. Among the developing G20 nations, the Former Soviet Union (FSU) and India experience the largest relative increases of

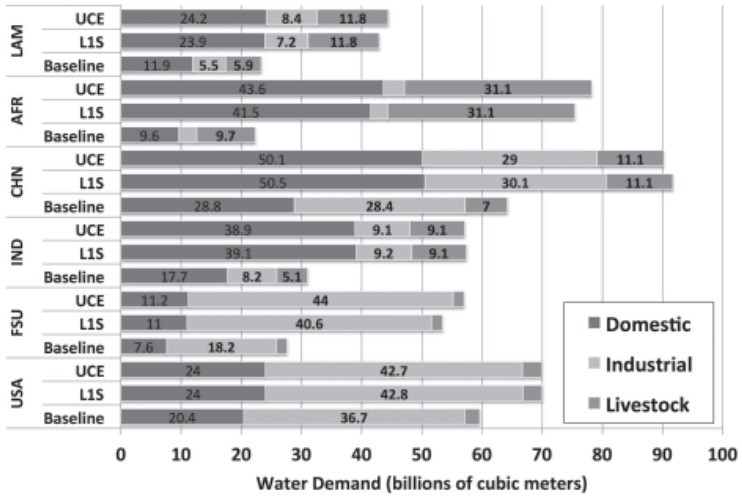

Figure 8. Nonirrigation water requirements. Shown are the totals for nonirrigation annual water demand (billion m^3/yr) from 2001 to 2010 for the baseline and 2041–2050 for the UCE, and L1S scenarios. The ASR-level data are aggregated from the EPPA regions (see Figure 1 and Table 2) to the developed, other G20 nations, and developing nations.

about 50%. In absolute terms, China's increases in demand are comparable (26 billion m^3/year), but in relative terms its increase is 40% from its baseline value. Generally speaking, developing nations roughly double their nonagricultural water demands. The one notable exception is Africa, which experiences a nearly fourfold increase in water demand. The effect of slower growth under the L1S scenario provides a marginal buffering of this increase, with total water requirements about 5% less compared with the UCE scenario.

Nevertheless, these comparative increases in water demand between developed and developing nations are in striking contrast to the projected changes in GDP. As shown in Table 2, while growth rates are similar or lower, the largest absolute changes in GDP are found in developed nations (such as the United States, Japan, and Europe), with much smaller absolute changes found in Africa, India, and China. These absolute differences reflect slower rates of growth in developed nations but from a much higher base level of GDP at present. This dichotomous relationship among nations between changes in water demands and GDP growth results from the statistically estimated relationships in the WRS between various water demands (industrial and municipal) and GDP that show plateauing demand at higher levels of economic activity [see *Strzepek et al*., 2013].

3.2.2. Global and Regional Climate Change

Next, we consider the simulations that single out the effects of trends in climate (i.e., precipitation, temperature, and runoff) on the modeled water stress, and the interplay of climate policy and uncertainties in regional patterns of change. For a global aggregate, we find that uncertain regional climate change has a much greater influence on water stress than the effect of the emission scenario on climate change. These results are shown in Figure 9, which tracks global water stress (shown as successive 5 year mean values) out to 2050. Figure 9a shows the global result if the ASRs are weighted by their total water use. In this picture, water stress is lowered through 2050 under the relatively WET climate pattern trend. However, the DRY climate pattern trend produces a monotonic increase in water stress over the period.

Additional insights are gained if the water-use weighting is removed from the global averaging (Figure 9b). For the unweighted case, both the wet and dry patterns both show increasing trends in water stress. In addition, their trends are larger than for the weighted case. This difference between the weighted and unweighted averaged results indicates that: (1) the majority of the ASRs that contain largest increases in WSI through the period have relatively low total withdrawals through 2050; and (2) for the WET scenarios, ASRs with higher withdrawal rates experience decreases in water stress through 2050 (illustrated in results below). In all these cases, the choice of the climate policy scenario (UCE or L1S) has

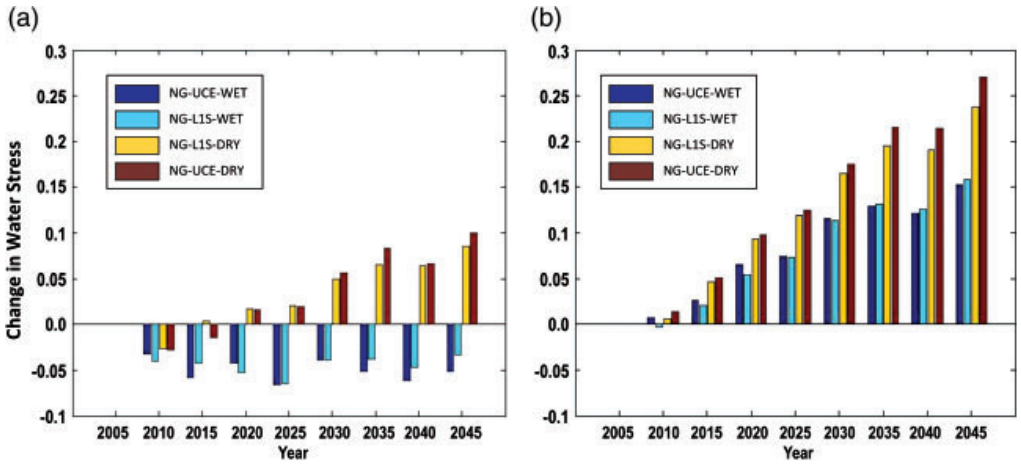

Figure 9. Trends in global water stress from climate factors. The change in water stress index, WSI (unitless), is shown as the difference in successive 5 year running means from the 2005–2009 average value. The global values are derived from ASR values that are: (a) weighted or (b) unweighted by its total annual withdrawal. The simulations assume no-growth (NG) in human water demands and thus highlight the effect of climate change as a result of unconstrained emissions (UCE) and a stabilization policy (L1S) as well as the effect of different regional climate change patterns (DRY and WET). Refer to Table 1 and corresponding text for further details regarding the suite of simulations performed.

a relatively small effect on the global WSI trends compared with the choice of the climate pattern trends or the choice of weighted averaging. It is important to note that, because of the influence of emissions before 2000 and climate inertia, the relative importance of the policy choice is expected to be greater if the simulation were extended to decades beyond 2050.

These characterizations are further reflected in the regional changes in the water stress among the ASRs (Figure 10). The larger regional difference in WSI trends among the scenarios is between the WET and DRY cases (comparing top and bottom maps in the figure), with smaller impacts observed in the choice between the UCE or L1S emission scenarios (left and right maps in the figure). The strongest increases in water stress are found in Africa, and the magnitude of these trends is reduced considerably when going from the DRY to WET climate pattern. As noted above, decreases in water stress are found for a number of ASRs with high withdrawal rates (e.g., the United States and China), in particular for the DRY cases. These features confirm the effects of weighted average observed in the global WSI trends (seen in Figure 9)

Among the main drivers of water stress, the regional features of runoff resonate strongly with the WSI trends. In particular, the majority of the largest relative decreases in runoff (Figure 11) are in African ASRs, and these correspond strongly with increases in WSI (i.e., greater water stress). Additionally, the increases and decreases in runoff observed in many ASRs over Europe and the United States show a consistent WSI response. Overall, the geographic texture in these runoff changes is affected notably by the choice of the WET or DRY pattern scenario, and again less than by the choice of emission scenario.

Another driver in the climate-driven trend on water stress is irrigation demand, which is responsive to the trends in precipitation and temperature within the ASR (both of which are modified through the climate change pattern-scaling approach employed). While changes in the irrigation consumption show notable differences in their regional features between the WET and DRY pattern scenario (Figure 12), these impacts are less prominent over Africa and more notable over Eurasia, Southeast Asia, as well as western parts of North America. The small effect of irrigation requirements on the most stressed areas, such as Africa, occurs because the area of irrigated land there is now small (and it is held constant over the simulation period). For most African ASRs, changes in runoff, not irrigation demand, are the main contributor to changes in water stress.

3.3. Integrated Projections Including Economic Growth and Climate Change

We consider the combined effect of economic growth and regional climate change (considered separately in the previous sections) on water stress. Figure 13a shows the global WSI trends with the ASRs weighted by their total water use, and Figure 13b shows the unweighted results. A comparison with Figure 9, which

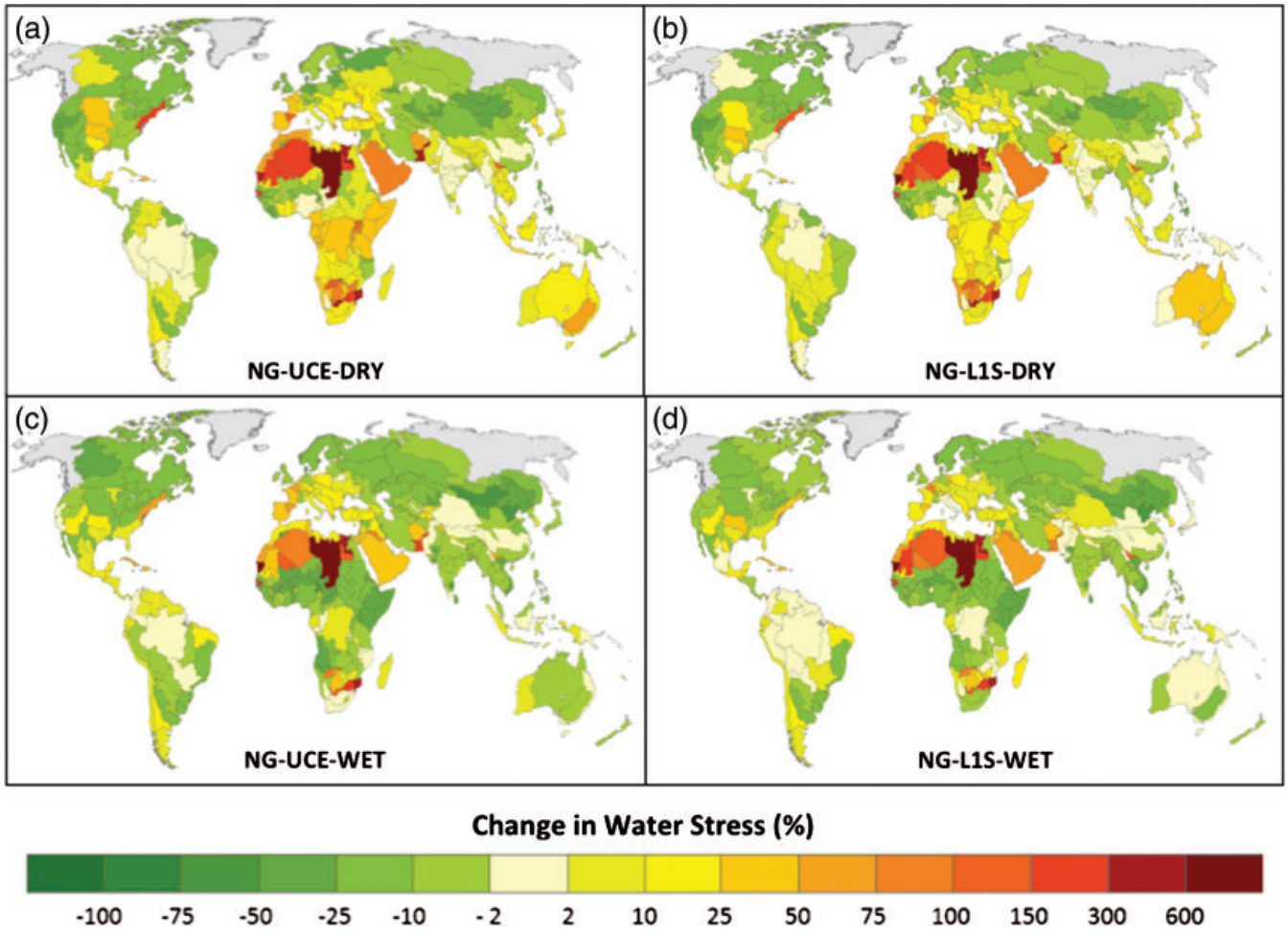

Figure 10. Changes in ASR water stress from climate factors. Maps show percentage changes in decadal averaged ASR water stress index, WSI, from 2001–2010 to 2041–2050. The simulations highlight the effect of climate change only (i.e., the "no-growth" scenarios denoted by NG in Table 1) as a result of unconstrained emissions (UCE) and a stabilization policy (L1S), as well as the effect of different regional pattern change scenarios (WET and DRY). With no-growth in the economic factors, these presented water stress changes are the result of only imposed changes in the climate forcing. Refer to Table 1 and corresponding text for further details regarding the suite of simulations performed.

shows climate effects only, demonstrates that at global scale economic growth is at least as strong a driver of changes in water stress through 2050 as climate. In all combinations of the emission and pattern change scenarios considered (UCE, L1S, WET, and DRY), the magnitude of the global water stress trend shows at least a doubling compared with the climate-only results (Figure 9) by 2050, and for the case of ASR-weighted WET cases (Figure 13a versus Figure 9a) the trend is reversed in sign (from negative to positive). In all cases, economic growth increases water stress globally.

However, consistent with the results considering the climate pattern scenarios alone, the WET pattern case is able to buffer the increase in water stress imposed by increasing water demands from economic growth. This effect shows up most dramatically in the case with ASR weighting by water use (Figure 13a), where the increase in water stress to 2050 in the DRY scenario is more than double that under the WET scenario. The same effect, though much reduced in scale, is observed when the weighting is removed (Figure 13b). As seen previously in the climate change-only results (Figure 9), the choice of the UCE or L1S policy scenario has a much smaller effect in a simulation limited to 2050. The overall implication of these results is that regional climate change uncertainty is a more influential factor in water stress trends than the global scale differences in the two climate policy scenarios.

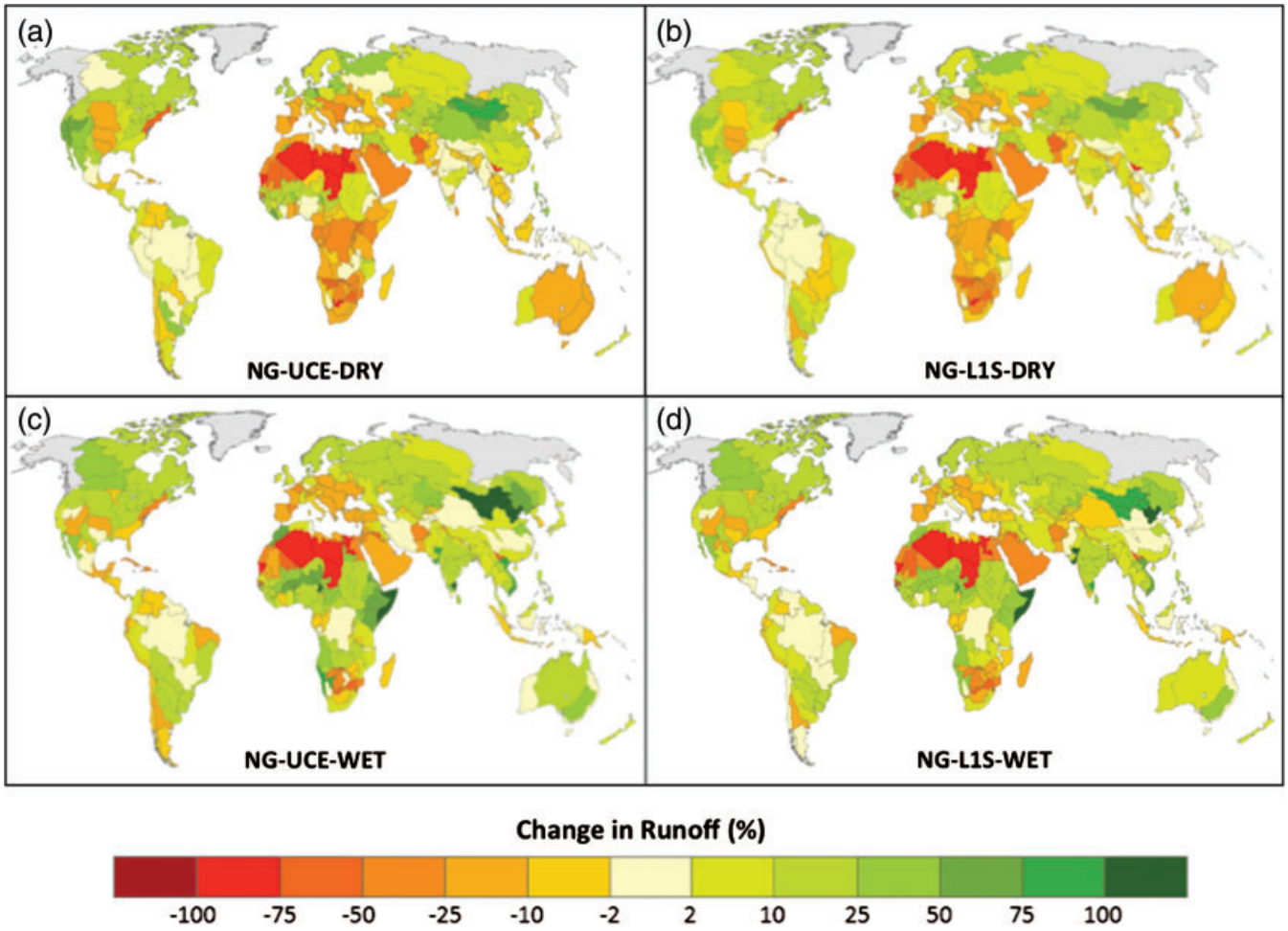

Figure 11. Changes in ASR runoff. Maps show percent changes in decadal averaged ASR runoff from 2001–2010 to 2041–2050. The simulations show the effect of climate change only (i.e., the "no-growth" scenarios denoted by NG in Table 1) as a result of unconstrained emissions (UCE) and a stabilization policy (L1S) as well as the effect of different regional pattern change scenarios (WET and DRY). Refer to Table 1 and corresponding text for further details regarding the suite of simulations performed.

Given these global trends in WSI, it is not surprising that many ASRs experience increases in water stress for both of the policy scenarios as well as the regional climate outcomes (Figure 14). The strongest (relative) increases in water stress are observed predominantly in Africa. However, strong relative increases (30% to over 100%) are also found in developed regions over North America and Europe. Due to the strong influence of nonagricultural water demand via socioeconomic growth (Figure 7) on the water stress trends, differences in the water stress change (by 2050) as a result of the different climate pattern change scenarios is not as clearly discernable as that observed in the NG case (Figure 10). Nevertheless, the WET pattern provides a buffering effect to the water stress increases in the Eastern United States, Australia, and throughout Africa and the Middle East. In Eastern and Southeast Asia, the WET pattern also enhances the reduction in water stress through 2050.

Among the more compelling regions is Southeast Asia. In this region, the most prominent features are reduced stress along the Yellow and Xi Jang Rivers in China, and along the Ganges and Bhramaputra basins in India—particularly in the WET case scenarios. These increases in water availability over China and India are encouraging given their high water stress conditions in the contemporary climate and built environment (Figure 5). Conversely, we also find increased water stress in a number of ASRs across India, the Indus River, Vietnam, and eastern China—particularly for the UCE-DRY case. These decreases can be buffered or reversed in the WET pattern scenario.

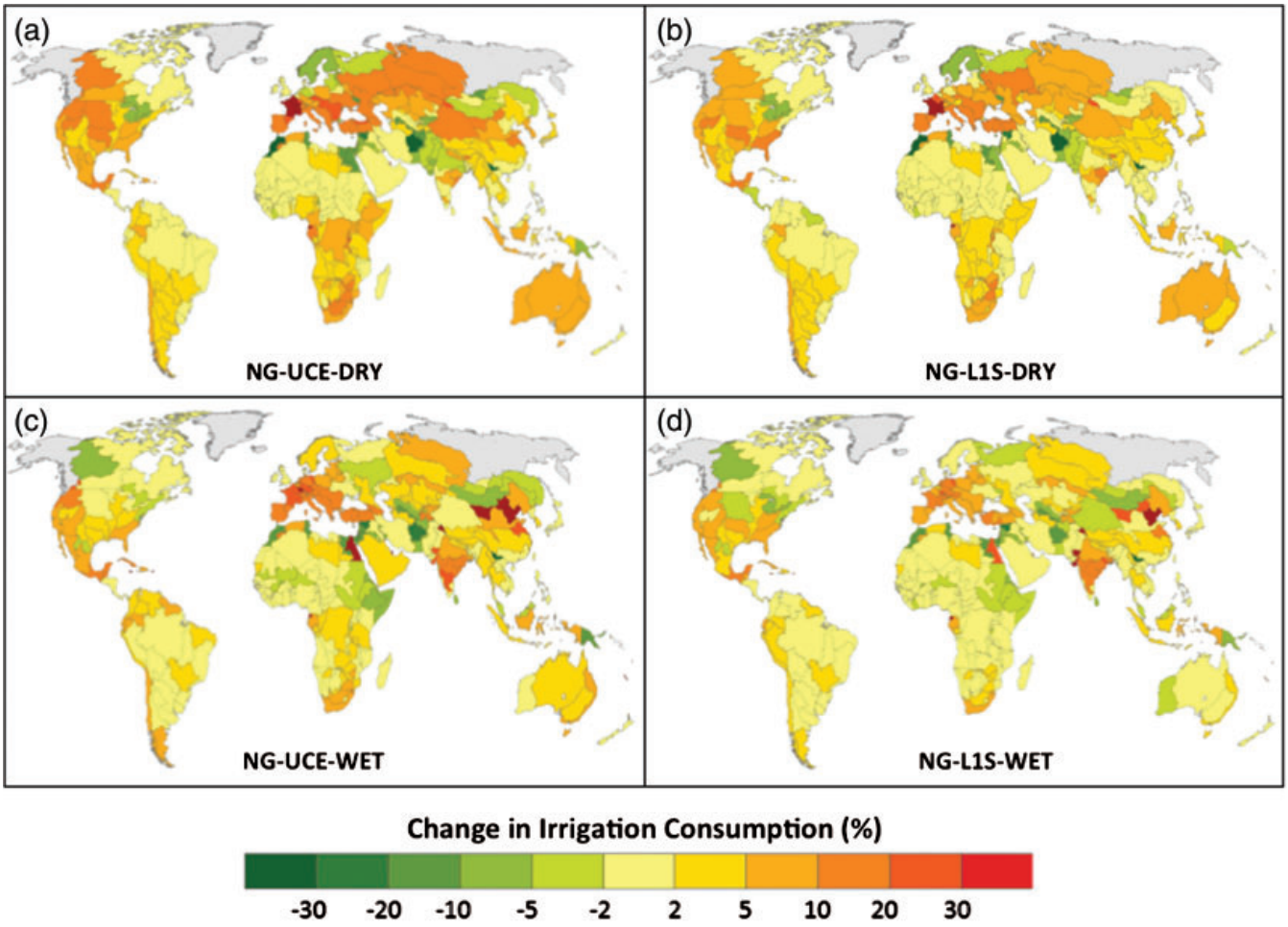

Figure 12. Changes in irrigation requirement from climate factors. Maps show percentage changes in decadal averaged irrigation consumption by ASR from 2001–2010 to 2041–2050 for the ASRs within the IGSM-WRS. With changes in irrigated area, the simulations highlight the effect of climate change as a result of unconstrained emissions (UCE) and a stabilization policy (L1S) as well as the effect of different regional pattern change scenarios (WET and DRY). Refer to Table 1 and corresponding text for further details regarding the suite of simulations performed.

Looking closer at the WSI changes in 2050 for various regions across the globe (Figure 14), we find that at the ASR levels, there is not a homogeneous regional impact with respect to the global scale hydroclimate characterizations (i.e., WET and DRY cases). In a number of instances, the change in WSI does not consistently follow the WET and DRY characterizations—as determined by the global land-only CMI trends. We find that WSI can increase under the global WET scenario. For example, under both the UCE and L1S scenarios, the Tibetan Plateau as well as basins across most of South America and central Eurasia shows increased water stress in the WET cases (Figures 14c and 14d). Conversely, the Chang Jiang and Yangtze rivers as well as across the western United States show decreased water stress under the DRY scenarios (Figures 14a and 14b). These results underscore the caveat that metrics designed to characterize the range of global scale hydroclimate conditions will not consistently capture all regional variations accordingly. Therefore, any risk-based assessment that aims to span the full range of hydroclimate outcomes must carefully consider the domain and metrics chosen.

3.4. Global Population at Risk to Water Stress

An analysis was performed to assess the population that is prone to water-stress exposure under current conditions and future scenarios (Table 1). Each ASR was assigned by its WSI to one of the water stress classifications as described in Section 2 (and shown in Figure 4). All ASRs whose values of WSI classified them in the moderately to extremely exploited (i.e., WSI > 0.3) category were deemed as exposed to "water

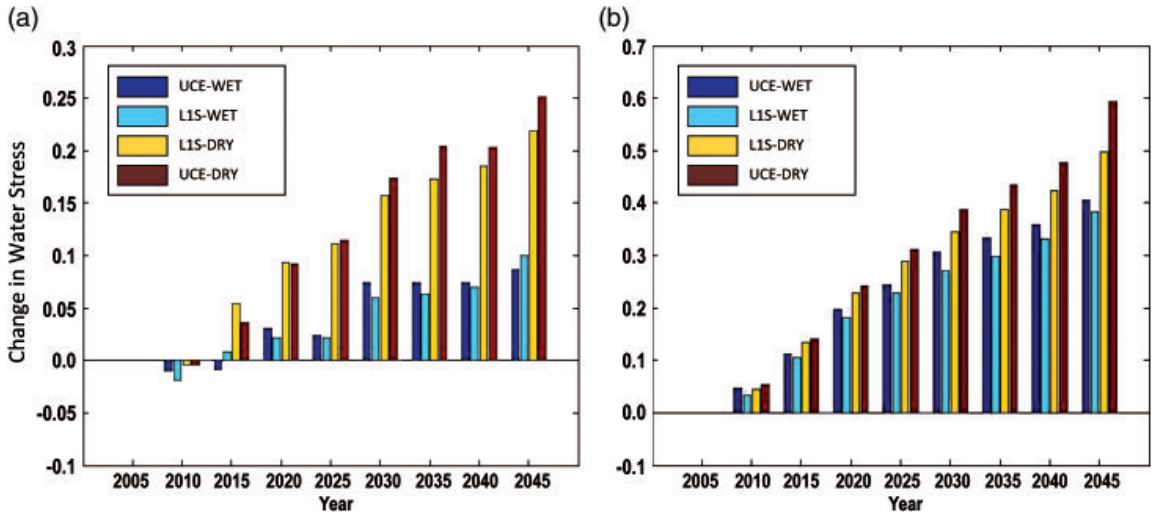

Figure 13. Trends in global water stress index (WSI). Shown is the change in global water stress index, WSI (unitless), obtained as the difference in successive 5 year running means from the 2005–2009 average value. The abscissa labels refer to the starting point of the 5 year running mean result. The global values shown are derived from ASR values that are: (a) weighted or (b) unweighted by total annual withdrawal. The WSI changes consider growth in human water demands over the period (e.g., Figures 6 and 7) as well as climate change effects (e.g., Figures 8–11) as a result of unconstrained emissions (UCE) and a stabilization policy (L1S) as well as the effect of different regional climate pattern scenarios (WET and DRY). Refer to Table 1 and corresponding text for further details regarding the suite of simulations performed. Note also the difference in vertical scale between the two panels.

stress" and tabulated according to their population. These tabulations were performed for the baseline conditions (i.e., Figure 4) and for each of the 11 future scenarios (as depicted in Figures 9 and 13). The populations in the "water-stressed" ASRs were aggregated globally as well by developing and OECD nations, and the results are summarized in Table 3 and Figure 15.

Overall, the impact of socioeconomic growth far exceeds that of climate change in terms of increasing risks to water stress. In absolute terms, the increases in population exposed to "water-stressed" conditions as a result of socioeconomic growth (the two HC scenario results in Table 3) are at least an order of magnitude higher than any change in the climate change-only scenarios (the NG scenario results of Table 3). They also show that overwhelmingly for any scenario, at least 80% of the water-stressed population shifts occur within the contemporary developing countries. We find that uncertain climate change, particularly for the UCE case, has a much stronger impact on these population-under-water-stress figures as compared with the range of socioeconomic growth under between the two emission scenarios (UCE and L1S). A difference of 350 million people, globally, between the WET and DRY cases under the UCE scenario is observed as compared with only 7 million between the UCE-HC and L1S-HC scenarios.

Globally, the combined effects of socioeconomic growth and climate change indicate that, by 2050, the population at risk of exposure to at least a moderate level of water stress could reach at least 5 billion people (Figure 15) under all four scenarios (UCE-WET, UCE-DRY, L1S-WET, and L1S-DRY). Furthermore, of this 5 billion people, up to 3 billion could be exposed to overly exploited conditions, which indicate that at the scale of the basins considered in the WRS global framework, the projections indicate that water requirements will consistently exceed the managed surface water supply. The population at 2050 under this overly exploited water stress are nearly double the current estimate (~1.7 billion people), and among the future scenarios it represents a range of increase between 1.0 and 1.3 billion people—with the range largely attributed to the choice between the WET and DRY cases (Figure 15). As noted above, the impact of climate policy does very little to buffer these increases (by comparing, e.g., the UCE-HC to the L1S-HC results). Although the effect is small, all WET cases show the reduction in the total population under water stress, most notably for the UCE-WET scenario—which can reduce the global population under overly exploited water stress by approximately 250 million as compared with the UCE-DRY case.

In considering these population-under-stress projections, we find that some of the largest increases in population (Table 4) occur in areas that are already under water stress, in particular, India, the Middle East (or MES region of EPPA), and Northern Africa (Figures 3 and 5). The total projected population increases

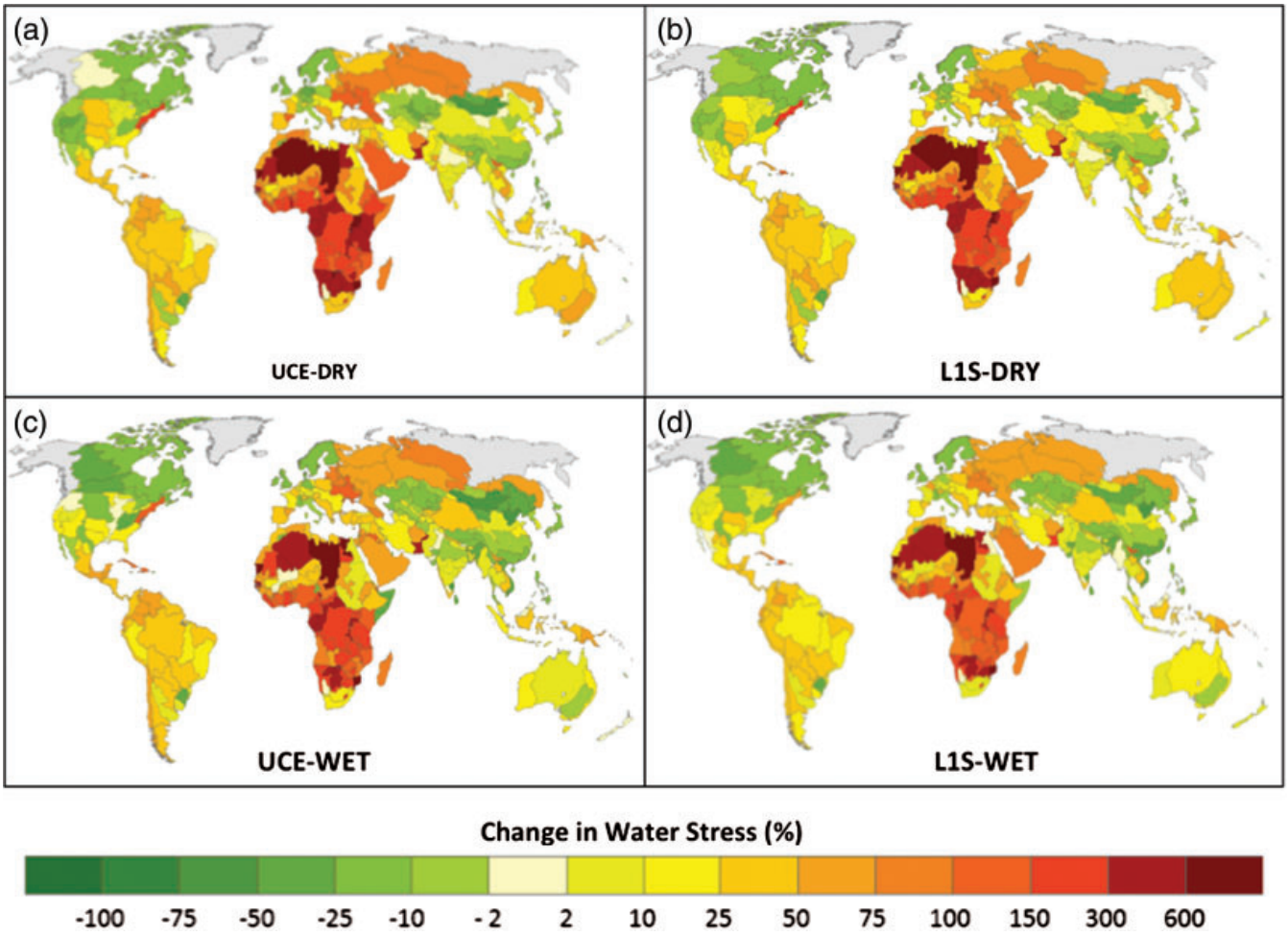

Figure 14. Changes in ASR water stress index (WSI). Maps show changes in decadal averaged ASR water stress from 2001–2010 to 2041–2050. The simulations highlight the effect of climate change as a result of unconstrained emissions (UCE) and a stabilization policy (L1S) as well as the effect of different regional patterns of climate change (WET and DRY). Refer to Table 1 and corresponding text for further details regarding the suite of simulations performed.

within these water-stressed regions, approximately 1.8 billion, could account for a substantial portion (up to 90%) of the nearly 2 billion people increase in water-stressed populations shown in Figure 15. A closer inspection indicates that given the increasing trends in WSI over the Middle East across all scenarios (Figure 14) and that none of the decreases in WSI observed over India are enough to diminish its water-stressed condition—all of the additional 660 million people projected to live in these regions (by 2050) will be exposed to water stress.

The situation for Africa is not as straightforward. The contemporary water stress estimate (Figure 5) shows that much of equatorial and subtropical Africa is experiencing only slight water-stressed conditions. However, the large population increase contributes to the substantial growth in nonagricultural water demands (Figure 7), and combined with the modest GDP growth (Table 2) and increases in irrigation consumption, particularly under the DRY scenarios, all of these regions in Africa experience increases in water stress that are large enough, in most cases, to be moved into the water-stressed categories shown in Figure 15. As a result, almost all of the additional 1.2 billion people (Table 4) are introduced into a water-stressed environment. In a similar fashion, China also presents an environment that is poised for expansive increase in water stress, given the large portion (over 50%) of its population in ASRs currently experiencing only slightly-to-moderately water-stressed conditions (Figures 3 and 5). These regions include the Xi Jang and Yangtze basins across southern China. However, in the scenarios considered, not only is China's population increase small compared with most EPPA regions (Table 4), but also these basins

Table 3. Changes in Population Exposed to Water Stress[a]

	Globe (3348)	Developing (2924)	OECD (424)
NG-UCE-WET	−137 (−4.1%)	−139 (−4.8%)	2 (0.4%)
NG-UCE-DRY	93 (2.8%)	33 (1.1%)	60 (14.1%)
NG-L1S-WET	−49 (−1.5%)	−92 (−3.2%)	43 (10.2%)
NG-L1S-DRY	60 (1.8%)	15 (0.5%)	45 (10.6%)
UCE-HC	1778 (53.1%)	1443 (49.4%)	335 (79.0%)
L1S-HC	1771 (53.0%)	1443 (49.4%)	328 (77.4%)
UCE-WET	1648 (49.2%)	1317 (45.0%)	331 (78.2%)
UCE-DRY	1993 (59.5%)	1633 (55.9%)	360 (85.0%)
L1S-WET	1654 (49.4%)	1337 (45.7%)	317 (74.8%)
L1S-DRY	1921 (57.4%)	1565 (53.5%)	356 (84.1%)

[a]Changes in total population (in millions) as well as percentage changes (in parentheses) across ASRs with a WSI greater than 0.3 (denoting moderately through extremely exploited water-stressed conditions). Changes were calculated as the difference between the 2001–2010 baseline conditions (given in parenthesis at each column heading) and the 2041–2050 periods. Results are shown for the simulations to highlight the effects of climate change-only (the NG scenario results) and economic growth separately (the HC scenario results). Refer to Table 1 for the nomenclature regarding the scenarios.

experience decreases in WSI and thus the population-under-stress increases are somewhat limited (less than 200 million)—relative to India, Africa, and the Middle East. Nevertheless, the aforementioned caveat concerning the representativeness of the WET and DRY cases, determined by a *global* moisture index, as representing the full range of hydroclimate outcomes for this region must be taken into account in a more comprehensive fashion. There may exist a number of drier outcomes for this region (not captured by the global CMI assessment) that would present a risk of these basins being pushed into a stressed environment. Additionally, the population and GDP growth scenarios considered are limited (due to computational demands) compared with the more comprehensive treatment of uncertainty provided by the IGSM [e.g., *Webster et al*., 2012]. In light of these issues, ongoing work with the IGSM-WRS is addressing

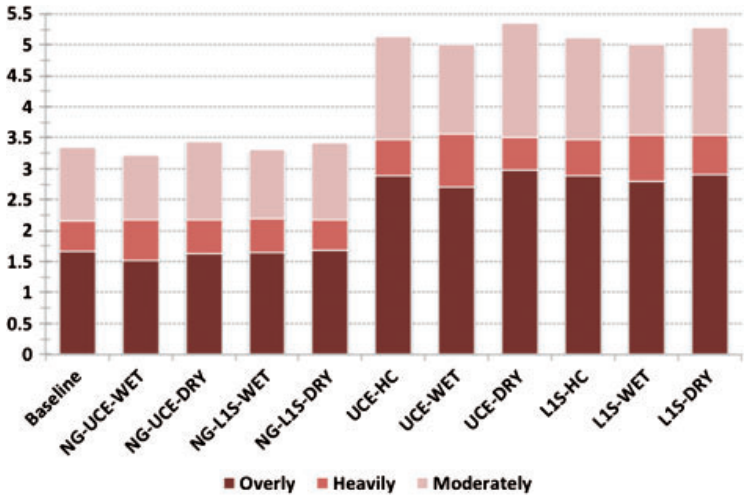

Figure 15. Global population exposed to water stress. The stacked bar chart displays the global population (in billions) exposed to water stress for the IGSM-WRS scenarios considered. Water stress is quantified by the water stress indicator (WSI) for each ASR, and each ASR's population is binned according to the WSI categories as depicted in Figure 4. The baseline result is based on 2001–2010 conditions, whereas all other scenarios show results for the period 2041–2050. The simulations highlight the effect of climate change and economic growth as a result of unconstrained emissions (UCE) and a stabilization policy (L1S) as well as the effect of different regional patterns of climate change (WET and DRY). Refer to Table 1 and corresponding text for further details regarding the suite of scenario simulations.

Table 4. Global Population[a]

		Population (millions)			
Major Regions	Region	2010	2050	2050–2010 Change	2050–2010 Change
Developed	ANZ	38.58	59.82	21.24	55.0
	CAN	35.35	47.86	12.51	35.39
	ROE	236.92	270.8	33.88	14.3
	EUR	538.37	582.13	43.76	8.1
	JPN	134.53	124.45	−10.08	−7.5
	USA	309.35	399.8	90.45	29.2
Other G20	CHN	1366.85	1404.45	37.6	2.75
	RUS	147.1	133.7	−13.4	−9.1
	BRA	197.83	237.89	40.06	20.2
	IND	1232.77	1736.23	503.46	40.8
	MEX	114.94	152.14	37.2	32.3
Developing	AFR	1026.54	2213.97	1187.43	115.7
	ASI	488.41	646.15	157.74	32.3
	LAM	284.61	400.96	116.35	40.9
	MES	217.05	379.29	162.24	74.5
	REA	619.09	883.99	264.9	42.8
Global total		6988.29	9673.63	2685.34	33.0

[a]Shown are the 2010 population, projections at 2050 (in millions), as well as absolute and percent changes (between 2010 and 2050) for the EPPA regions (denoted in Figure 2). Although only the 2010 and 2050 figures are shown, population projections were applied in the L1S and UCE scenarios (denoted in Table 1) for every year of the WRS runs to determine trends in nonagricultural water demands. For the no-growth (NG) runs, population was held fixed at the 2010 values.

these challenges (focused over Southeast Asia) to provide a more comprehensive risk-based assessment of future water stress for any region on interest.

4. Discussion and Closing Remarks

This study has employed the IGSM-WRS framework aimed at assessing the fate of managed water systems, depicted by 282 large basins across the globe. A suite of experiments was performed to assess the individual effects of socioeconomic growth and (uncertain) regional climate change over the coming decades. Additional experiments were also performed combining these drivers as well as considering two possible emission scenarios: one conveying an unconstrained emission pathway and the other a pathway to achieve stabilization of greenhouse gas concentrations by the end of the 21st century. Through these numerical experiments, we have quantified the trends over the coming decades (through 2050) in water stress, defined as a ratio of total water requirements over the available surface flow (from within-basin and upstream sources) across the network of managed, large water basins. Overall, the results highlight the substantial influence of socioeconomic growth on the global patterns of water stress, particularly in developing nations. Additionally, the factors that determine the sign and magnitude of water-stress response vary between major economic and developing regions. From the scenarios considered, we find that water stress changes within developed nations are more sensitive to climate drivers, whereas developing countries are far more responsive to socioeconomic growth. In addition, the results imply that the greatest risks to regions facing future water stress may not be captured by extreme outcomes from global assessments of climate scenarios, but rather by regional extremes occurring within a subset of climate model projections

Geographically, a number of salient results were found. By 2050, economic growth and population change alone may lead to an additional 1.8 billion people globally (a 53% increase) living in regions with high water stress. Of this additional 1.8 billion people, 80% are found in nations that are currently developing

countries. In comparison, impacts of climate change on the current population under a globally drier scenario may lead to an increase of 93 million people (a 2.8%) living in regions with high water stress, with the majority (60 million) of these located in developed nations. Under a globally wet scenario, climate change can lead to appreciable decreases (compared with the increases in the dry case) in water stress with an estimated 139 million fewer people under stress; however, these decreases are observed primarily in developed nations. Combined, the suite of these projections estimates that by 2050, as many as 5.0 of the 9.7 billion people (or 52% of the global population) in the world may be living under at least moderately stressed water resource conditions. Moreover, within this 5.0 billion is a 1.0–1.3 billion increase of the world's 2050 projected population living in regions with overly exploited water conditions—where total potential water requirements will consistently exceed surface water supply. Under the context of the WRS model framework, this would imply that adaptive measures would be taken to meet these surface water shortfalls and would include: water-use efficiency, reduced and/or redirected consumption, recurrent periods of water emergencies or curtailments, groundwater depletion, additional interbasin transfers, and overdraw from flow intended to maintain environmental requirements.

These populations-under-stress projections provide additional insights and also underscore some of the aforementioned findings. First and foremost, the strongest driver in these projections is the fact that a large portion of the population trends implemented in this study place people in basins that are already under water stress, most notably India, Northern Africa, and the Middle East. Furthermore, the range of socioeconomic trends that result from the emission policies considered has little effect on the additional populations exposed to water stress. However, on a global scale, the range and extent of possible climate pattern changes can play a secondary role to the effects of socioeconomic growth. As previously noted, we found that water stress changes were more sensitive, in developed nations, to the range of regional climate change. However, due to the higher populations (as well as their changes) in developing nations as compared with developed, we find that their sensitivity for these population-based water stress metrics are now quite comparable. There may very well be regional-to-local hotspots that amplify (or reverse) these comparative assessments. However, the scale of the basins (282 for the globe) employed for this particular study precludes an assessment as to the extent of these instances. Next, we discuss development and future work aimed to address this and other issues.

Several features in the design of this study must be noted that not only place the scope of the interpretations made, but also serve as guidance to further numerical experimentation and policy assessment. First, these numerical experiments consider how water stress would change under the contemporary built and managed environment. This is an important step prior to undertaking feasibility studies—to first identify where these risks may emerge under the current landscape and the underlying causes of these increased stresses. As such, we have yet to consider changes in infrastructure (e.g., energy systems), uncertain or alternative population projections, installed water storage capacity, cultivated land use, or irrigated area. Such adaptive measures will play an important role in preparing and/or avoiding future risks. Additionally, we have noted the fact that the characterization of (global) WET and DRY pattern cases may not necessarily align with the regional water stress impact response (i.e., it could be opposite in sign). Any global analysis of the risk of environmental change to water resources must be carried out as a collection of regional risk assessments that are then collated to a global coverage. In the global analysis, tradable commodities, such as food and agricultural products or energy (hydro and biofuels), that consume water must also be tracked to capture the simultaneous regional difference in impacts that may be lessened or exasperated by global trade.

Given these considerations, this model can next be used to focus on specific areas of the globe—e.g., East Asia, Southern Africa, and the western United States—to conduct more detailed simulations of future conditions and to undertake more rigorous assessments of future risks to water systems. For example, regional detail, such as water-use law and other restrictions on existing or planned interbasin transfers, can be introduced into the WSM component of the IGSM-WRS model. Adjustments in irrigated acreage, or in cropping patterns, can also be explored, and as previously noted, efforts to develop the model framework to provide self-consistent projections of irrigated land area that considers socioeconomic drivers, environmental pressures, and global-to-national governance—as well as their interactions—are ongoing. The impact of flexible design in future water systems can also be assessed. Future analyses will also

benefit from increased spatial scales of ASRs and further disaggregation of the nonagricultural water demand—especially in energy. To assess risks, large ensembles can also be performed, leveraging off the IGSM framework, that capture the spectrum of regional climate response, the range of climate policies, as well as the possible integrated changes in cultivated and irrigated lands. Combining all these elements in a consistent, integrated modeling framework presents a substantial computational undertaking but will ultimately result in persuasive and actionable insights for strategic planning and risk management in the face of unavoidable and preventable global change.

Acknowledgments

The Joint Program on the Science and Policy of Global Change is funded by the U.S. Department of Energy, Office of Science under grants DE-FG02-94ER61937, DE-FG02-93ER61677, DE-FG02-08ER64597, and DE-FG02-06ER64320; the U.S. Environmental Protection Agency under grants XA-83344601-0, XA-83240101, XA-83042801-0, PI-83412601-0, RD-83096001, and RD-83427901-0; the U.S. National Science Foundation under grants SES-0825915, EFRI-0835414, ATM-0120468, BCS-0410344, ATM-0329759, and DMS-0426845; the U.S. National Aeronautics and Space Administration under grants NNX07AI49G, NNX08AY59A, NNX06AC30A, NNX09AK26G, NNX08AL73G, NNX09AI26G, NNG04GJ80G, NNG04GP30G, and NNA06CN09A; the U.S. National Oceanic and Atmospheric Administration under grants DG1330-05-CN-1308, NA070AR4310050, and NA16GP2290; the U.S. Federal Aviation Administration under grant 06-C-NE-MIT; the Electric Power Research Institute under grant EP-P32616/C15124; and a consortium of 40 industrial and foundation sponsors (for the complete list see http://globalchange.mit.edu/sponsors/all). The authors thank Bilhuda Rasheed and Tony Smith-Greico for contributions to early versions of the manuscript.

References

Arnell, N. W., and S. N. Gosling (2013), The impacts of climate change on river flow regimes at the global scale, *J. Hydrol.*, *486*, 351–364, doi:10.1016/j.jhydrol.2013.02.010.

Blanc, E., K. Strzepek, C. A. Schlosser, H. Jacoby, A. Gueneau, C. Jant, S. Rausch, and J. Reilly (2013), Analysis of U.S. water resources under climate change, *Earth's Future*, *2*: 197–224. doi: 10.1002/2013EF000214/

Brown, A., and M. D. Matlock (2011), A review of water scarcity indices and methodologies, *Rep. 106*, April 2011, University of Arkansas - The Sustainability Consortium, p. 21.

Clarke, L., J. Edmonds, H. Jacoby, H. Pitcher, J. Reilly, and R. Richels (2007), *Scenarios of Greenhouse Gas Emissions and Atmospheric Concentrations. Sub-report 2.1A of Synthesis and Assessment Product 2.1 by the U.S. Climate Change Science Program and the Subcommittee on Global Change Research*. Department of Energy, Office of Biological & Environmental Research, Washington, D. C., 154 pp.

Döll, P, and J. Zhang (2010), Impact of climate change on freshwater ecosystems: A global-scale analysis of ecologically relevant river flow alterations, *Hydrol. Earth Syst. Sci.*, *5*(14), 783–799.

Fant, C., A. Gueneau, K. Strzepek, S. Awadalla, W. Farmer, E. Blanc, and C. A. Schlosser (2012): CliCrop: A crop water-stress and irrigation demand model for an integrated global assessment modeling approach. *MIT JPSPCG Rep. 214*, 26 pp., April. [Available at http://globalchange.mit.edu/files/document/MITJPSPGC_Rpt214.pdf.]

Food and Agriculture Organization of the United Nations (FAO) (2013), *FAO Statistical Yearbook 2013 – World Food and Agriculture*, FAO, Rome, Italy, isbn:978-92-5-107396-4 307 pp.

Fung, F., A. Lopez, and M. New (2011), Water availability in +2 degrees C and +4 degrees C worlds, *Philos. Trans. R. Soc. A Math. Phys. Eng. Sci.*, *369*(1934), 99–116.

Gao, X., C. A. Schlosser, A. Sokolov, K. W. Anthony, Q. Zhuang, and D. Kicklighter (2013), Permafrost degradation, methane and their biogeochemical climate-warming feedback, *Environ. Res. Lett.*, *8*(3), 035014.

Gosling, S. N., D. Bretherton, K. Haines, and N. W. Arnell (2010), Global hydrology modelling and uncertainty: Running multiple ensembles with a campus grid, *Philos. Trans. R. Soc. A Math. Phys. Eng. Sci.*, *368*(1926), 4005–4021.

Hirabayashi, Y., S. Kanae, S. Emori, T. Oki, and M. Kimoto (2008), Global projections of changing risks of floods and droughts in a changing climate, *Hydrol. Sci. J.*, *53*(4), 754–772.

IGFAGCR (2011): The Belmont Challenge: A global, environmental research mission for sustainability, 17 pp., March. [Available at https://igfagcr.org/sites/default/files/documents/belmont-challenge-white-paper.pdf.]

Meehl, G. A., C. Covey, T. Delworth, M. Latif, B. McAvaney, J. F. B. Mitchell, R. J. Stouffer, and K. E. Taylor (2007), The WCRP CMIP3 multi-model dataset: A new era in climate change research, *Bull. Am. Meteorol. Soc.*, *88*, 1383–1394.

Okazaki, A., J. F. Y. Pat, K. Yoshimura, M. Watanabe, M. Kimoto, and T. Oki (2012), Changes in flood risk under global warming estimated using MIROC5 and the discharge probability index, *J. Meteorol. Soc. Jpn.*, *90*(4), 509–524.

Oleson, K. W., et al. (2004), Technical description of the Community Land Model (CLM). National Center for Atmospheric Research, *Tech. Note NCAR/TN-461+STR*, 173 pp.

Rosegrant, M., C. Ringler, S. Msangi, T. Sulser, T. Zhu, and S. Cline (2008), *International Model for Policy Analysis of Agricultural Commodities and Trade (IMPACT): Model Description*, International Food Research Institute, Washington, D. C.

Schlosser, C. A., X. Gao, K. Strzepek, A. Sokolov, C. E. Forest, S. Awadalla, and W. Farmer (2012), Quantifying the likelihood of regional climate change: A hybridized approach, *J. Clim.*, *26*(10), 3394–3414, doi:10.1175/jcli-d-11-00730.1.

Schlosser, C.A., D. Kicklighter and A. Sokolov (2007): A Global Land System Framework for Integrated Climate-Change Assessments, *MIT JPSPGC Rep 147*, 60 pp., May. [Available at http://web.mit.edu/globalchange/www/MITJPSPGC_Rpt147.pdf.]

Siebert, S., P. Doll, J. Hoogeveen, J.-M. Faures, K. Frenken, and S. Feick (2005), Development and validation of the global map of irrigation, *Hydrol. Earth Syst. Sci.*, *9*, 535–547. sref:1607-7938/hess/2005-9-535.

Siebert, S., V. Henrich, K. Frenken, and J. Burke (2013), Update of the digital Global Map of Irrigation Areas (GMIA) to Version 5. Institute of Crop Science and Resource Conservation, Rheinische Friedrich-Wilhelms-Universität Bonn, Germany, 171 pp.

Smakhtin, V., C. Revanga, and P. Doll (2005), Taking into account environmental water requirements in global scale water resources assessments. [Available at http://www.iwmi.cgiar.org/assessment/files/pdf/publications/researchreports/carr2.pdf.]

Sokolov, A. P., et al. (2005), The MIT Integrated Global System Model (IGSM) Version 2: Model description and baseline evaluation. MIT JPSPGC *Rep. 124*, July, 40 pp. [Available at: http://globalchange.mit.edu/research/publications/696]

Strzepek, K., and C. A. Schlosser (2010), Climate change scenarios and climate data, *Development and Climate Change World Bank Discussion Paper #9*, October 2010, 26 pp.

Strzepek, K., C. A. Schlosser, A. Gueneau, X. Gao, É. Blanc, C. Fant, B. Rasheed, and H. Jacoby (2013), Modeling water resource systems under climate change: IGSM-WRS, *J. Adv. Model. Earth Syst.*, *5*(3), 638–653, doi:10.1002/JAME.20044.

Tang, Q. H., and D. P. Lettenmaier (2012), 21st century runoff sensitivities of major global river basins, *Geophys. Res. Lett.*, *39*, L06403, doi:10.1029/2011GL050834.

Thenkabail, P. S., et al. (2008), A Global Irrigated Area Map (GIAM) using remote sensing at the end of the last millennium, International Water Management Institute, 63 pp. [Available at: http://www.iwmigiam.org/info/gmi-doc/GIAM-world-book.pdf]

United Nations (UN) (2013), *World Population Prospects: The 2012 Revision*, Population Division, United Nations Department of Economic and Social Affairs. [Available at http://esa.un.org/unpd/wpp/Excel-Data/population.htm.]

United Nations World Water Assessment Programme (WWAP) (2014), *The United Nations World Water Development Report 2014: Water and Energy*, UNESCO, Paris, France 230 pp.

Vörösmarty, C. J., P. Green, J. Salisbury, and R. B. Lammers (2000), Global water resources: Vulnerability from climate change and population growth, *Science*, *289*, 284–288.
Wada, Y., L. P. H. van Beek, D. Viviroli, H. H. Dürr, R. Weingartner, and M. F. P. Bierkens (2011), Global monthly water stress: 2. Water demand and severity of water stress, *Water Resour. Res.*, *47*, W07518, doi:10.1029/2010WR009792.
Webster, M. D., et al. (2012), Analysis of climate policy targets under uncertainty, *Clim. Change*, *112*(3–4), 569–583.
Willmott, C. J., and J. J. Feddema (1992), A more rational climatic moisture index, *Prof. Geogr.*, *1*, 84–88, doi:10.1111/j.0033-0124.1992.00084.x.
World Commission on Dams (WCOD) (2000), *Dams and Development: A New Framework for Decision-Making – The Report of the World Commission on Dams*, Earthscan Publ., London, England 356 pp.

MIT Joint Program on the Science and Policy of Global Change - REPRINT SERIES

FOR THE COMPLETE LIST OF REPRINT TITLES: http://globalchange.mit.edu/research/publications/reprints

2013-34 European-Led Climate Policy versus Global Mitigation Action: Implications on Trade, Technology, and Energy, De Cian, E., I. Keppo, J. Bollen, S. Carrara, H. Förster, M. Hübler, A. Kanudia, S. Paltsev, R.D. Sands and K. Schumacher, *Climate Change Economics,* 4(Suppl. 1): 1340002 (2013)

2013-35 Beyond 2020—Strategies and Costs for Transforming the European Energy System, Knopf, B., Y.-H.H. Chen, E. De Cian, H. Förster, A. Kanudia, I. Karkatsouli, I. Keppo, T. Koljonen, K. Schumacher and D.P. van Vuuren, *Climate Change Economics,* 4(Suppl. 1): 1340001 (2013)

2013-36 Estimating regional methane surface fluxes: the relative importance of surface and GOSAT mole fraction measurements, Fraser, B., P.I. Palmer, L. Feng, H. Boesch, A. Cogan, R. Parker, E.J. Dlugokencky, P.J. Fraser, P.B. Krummel, R.L. Langenfelds, S. O'Doherty, R.G. Prinn, L.P. Steele, M. van der Schoot and R.F. Weiss, *Atmospheric Chemistry and Physics,* 13: 5697–5713 (2013)

2013-37 The variability of methane, nitrous oxide and sulfur hexaflouride in Northeast India, Ganesan, A.L., A. Chatterjee, R.G. Prinn, C.M. Harth, P.K. Salameh, A.J. Manning, B.D. Hall, J. Mühle, L.K. Meredith, R.F. Weiss, S. O'Doherty and D. Young, *Atmospheric Chemistry and Physics,* 13: 10633–10644 (2013)

2013-38 Integrated economic and climate projections for impact assessment, Paltsev, S., E. Monier, J. Scott, A. Sokolov and J.M. Reilly, *Climatic Change*, October 2013, doi: 10.1007/s10584-013-0892-3 (2013)

2013-39 Fiscal consolidation and climate policy: An overlapping generations perspective, Rausch, S., *Energy Economics,* 40(Supplement 1): S134–S148 (2013)

2014-1 Estimating a global black carbon emissions using a top-down Kalman Filter approach, Cohen, J.B. and C. Wang, *Journal of Geophysical Research—Atmospheres,* 119: 1–17, doi: 10.1002/2013JD019912 (2014)

2014-2 Air quality resolution for health impact assessment: influence of regional characteristics, Thompson, T.M., R.K. Saari and N.E. Selin, *Atmospheric Chemistry and Physics,* 14: 969–978, doi: 10.5194/acp-14-969-2014 (2014)

2014-3 Climate change impacts on extreme events in the United States: an uncertainty analysis, Monier, E. and X. Gao, *Climatic Change,* doi: 10.1007/s10584-013-1048-1 (2014)

2014-4 Will economic restructuring in China reduce trade-embodied CO_2 emissions? Qi, T., N. Winchester, V.J. Karplus, X. Zhang, *Energy Economics,* 42(March): 204–212 (2014)

2014-5 Assessing the Influence of Secondary Organic versus Primary Carbonaceous Aerosols on Long-Range Atmospheric Polycyclic Aromatic Hydrocarbon Transport, Friedman, C.L., J.R. Pierce and N.E. Selin, *Environmental Science and Technology,* 48(6): 3293–3302 (2014)

2014-6 Development of a Spectroscopic Technique for Continuous Online Monitoring of Oxygen and Site-Specific Nitrogen Isotopic Composition of Atmospheric Nitrous Oxide, Harris, E., D.D. Nelson, W. Olszewski, M. Zahniser, K.E. Potter, B.J. McManus, A. Whitehill, R.G. Prinn and S. Ono, *Analytical Chemistry,* 86(3): 1726–1734 (2014)

2014-7 Potential Influence of Climate-Induced Vegetation Shifts on Future Land Use and Associated Land Carbon Fluxes in Northern Eurasia, Kicklighter, D.W., Y. Cai, Q. Zhuang, E.I. Parfenova, S. Paltsev, A.P. Sokolov, J.M. Melillo, J.M. Reilly, N.M. Tchebakova and X. Lu, *Environmental Research Letters,* 9(3): 035004 (2014)

2014-8 Implications of high renewable electricity penetration in the U.S. for water use, greenhouse gas emissions, land-use, and materials supply, Arent, D., J. Pless, T. Mai, R. Wiser, M. Hand, S. Baldwin, G. Heath, J. Macknick, M. Bazilian, A. Schlosser and P. Denholm, *Applied Energy,* 123(June): 368–377 (2014)

2014-9 The energy and CO_2 emissions impact of renewable energy development in China, Qi, T., X. Zhang and V.J. Karplus, *Energy Policy*, 68(May): 60–69 (2014)

2014-10 A framework for modeling uncertainty in regional climate change, Monier, E., X. Gao, J.R. Scott, A.P. Sokolov and C.A. Schlosser, *Climatic Change,* online first (2014)

2014-11 Markets versus Regulation: The Efficiency and Distributional Impacts of U.S. Climate Policy Proposals, Rausch, S. and V.J. Karplus, *Energy Journal*, 35(SI1): 199–227 (2014)

2014-12 How important is diversity for capturing environmental-change responses in ecosystem models? Prowe, A. E. F., M. Pahlow, S. Dutkiewicz and A. Oschlies, *Biogeosciences*, 11: 3397–3407 (2014)

2014-13 Water Consumption Footprint and Land Requirements of Large-Scale Alternative Diesel and Jet Fuel Production, Staples, M.D., H. Olcay, R. Malina, P. Trivedi, M.N. Pearlson, K. Strzepek, S.V. Paltsev, C. Wollersheim and S.R.H. Barrett, *Environmental Science & Technology*, 47: 12557–12565 (2013)

2014-14 The Potential Wind Power Resource in Australia: A New Perspective, Hallgren, W., U.B. Gunturu and A. Schlosser, *PLoS ONE,* 9(7): e99608, doi: 10.1371/journal.pone.0099608 (2014)

2014-15 Trend analysis from 1970 to 2008 and model evaluation of EDGARv4 global gridded anthropogenic mercury emissions, Muntean, M., G. Janssens-Maenhout, S. Song, N.E. Selin, J.G.J. Olivier, D. Guizzardi, R. Maas and F. Dentener, *Science of the Total Environment,* 494-495(2014): 337-350 (2014)

2014-16 The future of global water stress: An integrated assessment, Schlosser, C.A., K. Strzepek, X. Gao, C. Fant, É. Blanc, S. Paltsev, H. Jacoby, J. Reilly and A. Gueneau, *Earth's Future*, online first (doi: 10.1002/2014EF000238) (2014)

For limited quantities, Joint Program Reprints are available free of charge. Contact the Joint Program Office to order.